Investigation of the molecular mechanism of Xiangsha Liujun Pill in the treatment of gastritis based on network pharmacology and molecular docking

Jiaen Wei (jiaenwei8@163.com)
Guangdong Medical University
Zhengxiu Li (lizhengxiu2021@163.com)
Guangdong Medical University
Tingting Tang (tingtingtang0430@163.com)
Guangdong Medical University
Ruolan Yu (ruolan_yu@163.com)
Guangdong Medical University
Xuejing Cao (caoxuejing0311@163.com)
Guangdong Medical University
Yong Liu (liuyong0614@126.com)
Guangdong Medical University
Zunnan Huang (zn_huang@gdmu.edu.cn)
Guangdong Medical University

Research Article

Keywords: Xiangsha Liujun Pill (XSLJP), Gastritis, Network pharmacology, Molecular docking, Action mechanism

DOI: https://doi.org/

Investigation of the molecular mechanism of Xiangsha Liujun Pill in the treatment of gastritis based on network pharmacology and molecular docking

Jiaen Wei[1#], Zhengxiu Li[1#], Tingting Tang[1#], Ruolan Yu[1], Xuejing Cao[2], Yong Liu[1], Zunnan Huang[1,3*]

[1] Key Laboratory of Big Data Mining and Precision Drug Design of Guangdong Medical University, Key Laboratory of Computer-Aided Drug Design of Dongguan City, Key Laboratory for Research and Development of Natural Drugs of Guangdong Province, Guangdong Medical University, Dongguan 523808, China.

[2] The Second Clinical Medical College of Guangdong Medical University, Dongguan 523808, Guangdong, China.

[3] Marine Medical Research Institute of Guangdong Zhanjiang, Zhanjiang, Guangdong 524023, China.

#These authors contributed equally to this work.

*Correspondence should be addressed to Zunnan Huang, zn_huang@gdmu.edu.cn, Guangdong Medical University, No. 1 Xincheng Road, Dongguan 523808, China. Tel.: +86 13925590670.

Abstract

Xiangsha Liujun Pill (XSLJP) is a traditional Chinese medical complex prescription containing ten herbs and is widely used to treat gastrointestinal diseases. This study aims to investigate the mechanism of XSLJP treating gastritis. We first identified 327 targets based on 118 active components using the TCMSP, SwissTargetPrediction and STITCH databases and 180 gastritis-related targets using the DisGeNET database. Their intersection revealed that 26 common targets may play crucial roles in gastritis therapy by XSLJP. Then, we identified 12 key active components and eight hub proteins from the 'drug-component-common target' network. Finally, KEGG and GO enrichment analyses revealed that the therapeutic targets of XSLJP were mainly related to inflammation and cancer pathways, such as TNF, JAK/STAT and MAPK signalling pathway. This study not only provides new ideas for further exploring the specific mechanism of XSLJP treating gastritis but also offers a theoretical basis for future research on its active components.

Key words

Xiangsha Liujun Pill (XSLJP); Gastritis; Network pharmacology; Molecular docking; Action mechanism

Introduction

Xiangsha Liujun Pill (XSLJP), which has been modified from Liujunzi decoction in the Orthodox Medical Record [1], the ancient herbal formulae of traditional Chinese medicine, is composed of 10 Chinese herbs, namely, *Radix Aucklandiae* (*RA*, *muxiang*), *Amomum* (*AM*, *sharen*), *Ginger* (*GI*, *shengjiang*), *Codonopsis* (*CO*, *dangshen*), *Atractylodes* (*AT*, *baizhu*), *Poria* (*PO*, *fuling*), *Glycyrrhiza* (*GL*, *gancao*), *Tangerine Peel* (*TP*, *chenpi*), *Pinellia* (*PI*, *banxia*), and *Jujube* (*JU*, *dazao*). In clinical therapeutics, XSLJP has been mainly used for dyspepsia, anorexia and abdominal distension [2], and combination treatments consisting of XSLJP and chemical drugs exert a significant therapeutic effect on the clinical treatment of chronic gastritis [3-5].

Many animal experiments and clinical trials have shown that XSLJP has

a certain curative effect on gastritis treatment. For example, Lin et al. explored whether XSLJP can improve the clinical symptoms and pathological changes of the gastric mucosa in rats with *Helicobacter pylori*-associated gastritis [6]. Huang et al. showed that XSLJP can effectively relieve the symptoms of patients with chronic renal failure and spleen kidney qi deficiency syndrome by improving their renal function and reducing the levels of hormones such as gastrin, motilin and somatostatin [7]. Ok et al. found that *Tangerine Peel* combined with *Pinellia* in XSLJP can effectively reduce the level of inflammatory factors in rats with inflammation [8]. In addition, molecular biology experiments have indicated that some active components in XSLJP can efficiently relieve gastritis-related symptoms. For instance, Liu et al. found that CMP33, a component of *Poria*, can significantly inhibit the lipopolysaccharide (LPS)-stimulated expression of IL-6, TNF-α and IL-1β to attenuate inflammation in RAW264.7 murine macrophage cells [9]. Ji et al. indicated that atractylenolide I (ATL-1), an active component of *Atractylodes*, exerts an anti-inflammatory effect on RAW264.7 cells by inhibiting the production of TNF-α and IL-6, and its underlying mechanism might be related to inhibition of the NF-κB, ERK1/2 and p38 signaling pathways [10]. Due to the complex mixture of components in XSLJP, its active and adverse components and its pharmacological mechanism remain unclear. Thus, systematic explorations of the active components and potential mechanisms of action of XSLJP in the treatment of gastritis are needed at the cellular and molecular levels.

Network pharmacology is characterized by its integral emphasis on multicomponent and multitarget therapy, which is exactly coincident with the holistic view of traditional Chinese medicine (TCM) [11]. Due to the rapid development of modern TCM databases and analysis methods, network pharmacology has become a bridge for the effective combination of TCM and modern medicine [11]. The study of TCM prescriptions through network pharmacology can not only fully analyze their important active components and mechanisms, but also promote the modernization of TCM [12]. For example, Huang et al. predicted the presence of 34 components with biological activity in Yinchenhao decoction, and these components mainly act on 31 pathways, as determined by network pharmacology [13]. Furthermore, these researchers speculated that the anticancer effect of these 34 components might be induced through regulation of cell death, energy metabolism, anti-inflammation, and anti-angiogenesis and suppression of the immune response [13]. This finding indicates that

network pharmacology might be a powerful analytical tool to study the mechanisms of various preparations of Chinese herbal medicines.

Therefore, based on network pharmacology, this study identified the active components of XSLJP and their therapeutic targets in the treatment of gastritis using four databases, namely, the TCMSP database [14] (http://tcmspw.com/tcmsp.php), the SwissTargetPrediction (STP) database [15] (http://www.swisstargetprediction.ch/), the STITCH database [16] (http://stitch.embl.de/) and the DisGeNET database [17] (https://www.disgenet.org/). The PubMed database (https://pubmed.ncbi.nlm.nih.gov/) was then utilized to retrieve experimental studies that confirm the identified active component-target pairs, and molecular docking simulations were performed using Discovery Studio (DS) software [18] to verify the putative active component-target pairs. Subsequently, a network diagram of the active components and disease targets was constructed using the STRING database [19] (https://string-db.org/) and Cytoscape [20] (https://cytoscape.org/) software, and from this network diagram, the key targets of and the important active components in XSLJP were determined according to various topology parameters. Furthermore, the important signaling pathways and biological processes of XSLJP were identified through KEGG pathway analysis and GO biological process analysis using the DAVID database [21] (https://david.ncifcrf.gov/). We then comprehensively analyzed and discuss the mechanism of action of XSLJP in the treatment of gastritis and provide a reference for further research on the development and utilization of traditional Chinese medicine resources. The entire workflow of this study is shown in Figure 1.

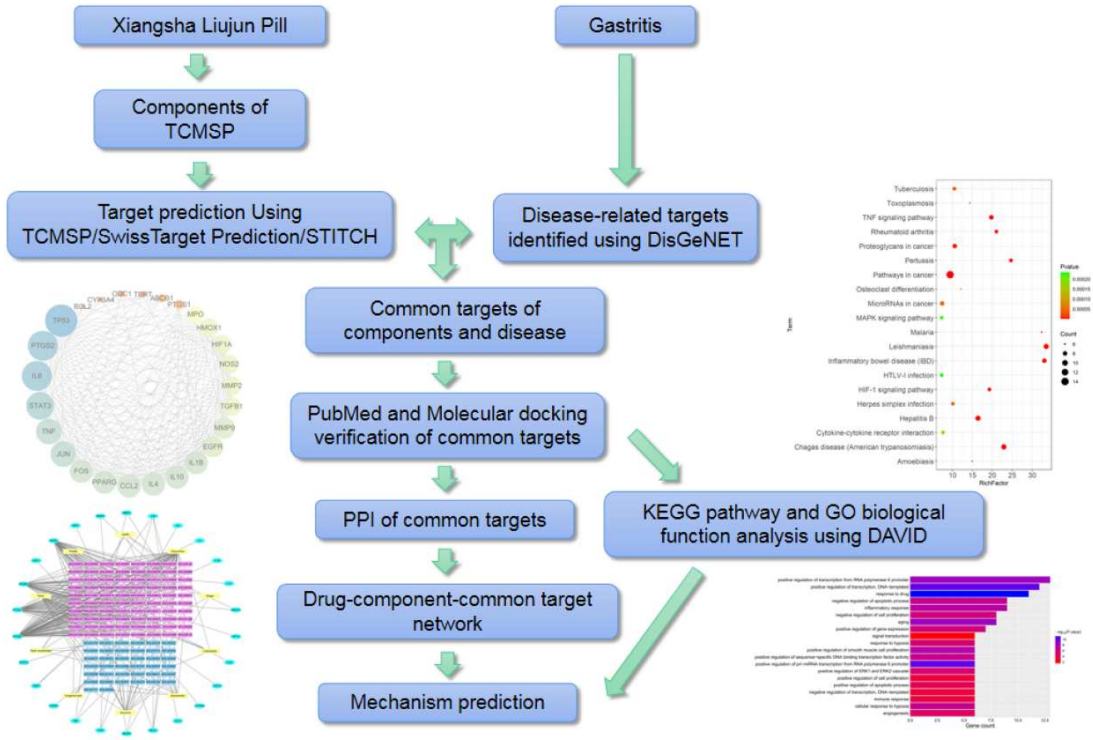

Figure 1: Complete workflow of this study.

Materials & Methods

Data collection

The TCMSP database [14] and the PubChem database [22] (https://pubchem.ncbi.nlm.nih.gov/), were used to collect the active chemical compounds of ten herbs in XSLJP and their structures, respectively. Based on their ADME parameters, the active components were identified according to the following criteria: oral bioavailability (OB) ≥ 30%, drug-like property (DL) ≥ 0.18, and half-life (HL) ≥ 4 h. Any duplicates were then removed.

The DisGeNET database [17] was searched using the keyword ‘gastritis’ to collect gastritis-related targets, and the sample ID used in the search was DisGeNET UMLS CUI: C0017152.

Target prediction and verification of active components

The TCMSP database [14], STP database [15] and STITCH database [16] were used for predicting and screening the targets of the active components. The predicted targets from the TCMSP database were identified based on the following criteria: OB ≥ 30%, DL ≥ 0.18, and HL ≥ 4 h. The predicted targets from the STP database were retrieved based on a probability greater than 0.3, and those from the STITCH database had a confidence value greater than 0.4.

After integrating and removing duplicated targets, the gene symbol of the predicted targets were obtained in the UniProt ID format using the UniProt [23] (http://www.uniprot.org) database. The common targets from the list of predicted targets and that of gastritis-related targets were then obtained.

The PubMed database was used for literature mining to identify information on the protein targets of the various TCM components. Although the protein targets of some active components were confirmed by literature records, the remaining common targets were further verified by molecular docking.

Network construction

The common targets were analyzed using the STRING database [19], and a protein-protein interaction network diagram (PPI) was obtained and then imported into Cytoscape 3.7.1 software [20]. Subsequently, we calculated the topological parameters, such as the degree, betweenness centrality and closeness centrality, of the PPI diagram for network screening and rendering to determine an appropriate or the best layout. Using Cytoscape, the key proteins with topological parameters higher than the average of all the nodes in the network were identified [20].

In addition, the drugs, components and common targets were imported into Cytoscape 3.7.1 software to obtain the ‘drug-component-common target’ network diagram, and a topological analysis using the degree value as the main reference standard was conducted to identify the key active

components [20].

Molecular docking

Discovery Studio software was used to simulate the interaction between molecules and to predict their binding pattern and affinity based on the receptor characteristics and the interaction modes between protein receptors and drug molecules [18]. The molecular structures of the active components were obtained from the PubChem database [22] (https://pubchem.ncbi.nlm.nih.gov/), and the crystal structures of the proteins were downloaded from the PDB database [24] (http://www.rcsb.org/).

Molecular docking between the active components and experimentally unverified targets was performed using the LibDock mode under the CHARMM force field [25]. The docking parameters were set as follows: docking tolerance, 0.25; energy threshold, 20.9; docking performance, high quality; construction method, FAST; minimization algorithm, intelligent minimum; and all other parameters, default values. Through computer calculation, a LibDock score is obtained, and a higher score indicates better docking. In addition, the molecular docking of key active components and hub protein targets was performed using the more accurate flexible docking mode, in which both the conformation of the active components and the amino acid residues at the binding sites of protein receptors can vary during the docking process [26]. In the flexible docking model, the result named -CDOCKER INTERACTION ENERGY is obtained [26]. A greater negative value of energy indicates a more stable docking interaction.

Pathway analysis

To obtain their enriched pathways and functions, the common target proteins were further investigated through Kyoto Encyclopedia of Genes and Genomics (KEGG) gene pathway analysis and Gene Ontology Database (GO) biological process analysis (BP) using the DAVID Biological Information Annotation database [21]. Using $P < 0.05$ as the screening criteria, the top 20 signaling pathways and top 20 biological processes with the lowest *P*-values obtained from the KEGG signaling pathway and GO

analyses, respectively, were selected.

Results

Active components in XSLJP and protein targets related to gastritis

In the TCMSP database, 122 compounds were screened through a search using the following keywords: *Radix Aucklandiae* (*RA*, *muxiang*), *Amomum* (*AM*, *sharen*), *Ginger* (*GI*, *shengjiang*), *Codonopsis* (*CO*, *dangshen*), *Atractylodes* (*AT*, *baizhu*), *Poria* (*PO*, *fuling*), *Glycyrrhiza* (*GL*, *gancao*), *Tangerine peel* (*TP*, *chenpi*), *Pinellia* (*PI*, *banxia*), and *Jujube* (*JU*, *dazao*). Because the main active ingredients of *RA* [27], *AM* [28] and *AT* [29] are volatile oils with important pharmacological activities, the screening conditions for these three medicines were relaxed and adjusted to "OB ≥ 30%, DL ≥ 0.1, and HL ≥ 1 h". Subsequently, 19 compounds, including one in *RA*, namely, cynaropicrin, 11 in *AM*, such as junipene and isospathulenol, and seven in *AT*, including atractylenolide I, atractylenolide II and atractylenolide III, were reincorporated in this study, and these were marked in Table 1S. The active components include six in *RA,* 20 in *AM*, three in *GI*, five in *CO*, 12 in *AT*, 15 in *PO*, 49 in *GL*, four in *TP*, three in *PI* and five in *JU.* After the duplicate compounds were deleted, a total of 118 active components were obtained, and these were shown in Table 1S.

Gastritis-related targets were collected using the DisGeNET database, and as shown in Table 2S, 180 targets were obtained using the keyword 'gastritis'.

Target prediction and literature-mining verification of active components

As shown in Table 3S, 327 targets were screened from the STP, STITCH and TCMSP databases based on the 118 active components using the standardization procedure and the UniProt database. According to their structures, the predicted targets can bind to the active component. The intersection among the predicted targets (Table 3S) and gastritis-related targets (Table 2S) yielded 26 common targets (Table 1), and these were

considered potential targets of XSLJP in the treatment of gastritis.

As shown in Table 4S, a literature search of the PubMed database showed that 21 of the 26 common targets can interact with the components of XSLJP, and these were thus considered verified targets. The remaining five common targets had not been validated in the literature and were thus considered unverified targets. Using Discovery Studio software, 118 active components (Table 1S) and the five unverified targets (Table 1) were successfully docked with a reasonable score under the LibDock mode, as shown in Table 5S. As a result, all 26 targets have been verified. A network diagram of the active components in XSLJP and 21 experimentally verified targets was constructed (Figure 2), and a network diagram of the active compounds and five computationally verified targets was also built (Figure 3).

Table 1: Information on the 26 common targets.

Target Name	Gene Name
Matrix metalloproteinase-2	MMP2
Heme oxygenase 1	HMOX1
Interleukin-10	IL10
Signal transducer and activator of transcription 3	STAT3
Prostaglandin G/H synthase 2	PTGS2
Interleukin-1 β	IL1B
Proto-oncogene c-Fos	FOS
Interleukin-4	IL4
Transcription factor AP-1	JUN
Peroxisome proliferator-activated receptor gamma	PPARG
Tumor necrosis factor	TNF
Cytochrome P450 3A4	CYP3A4
Interleukin-6	IL-6
Cellular tumor antigen p53	TP53
Epidermal growth factor receptor erbB1	EGFR
Prostaglandin G/H synthase 1	PTGS1
Apoptosis regulator Bcl-2	BCL2
Matrix metalloproteinase-9	MMP9
Chemokine (C-C motif) ligand 2	CCL2
Hypoxia-inducible factor 1-α	HIF1A
P-glycoprotein 1	ABCB1
Telomerase reverse transcriptase*	TERT
Nitric oxide synthase, inducible*	NOS2
Myeloperoxidase*	MPO
Transforming growth factor β-1*	TGFB1
Ornithine decarboxylase*	ODC1

Note: The asterisk (*) indicates that the target has not been verified by previous experiments, as determined by a search of the PubMed database.

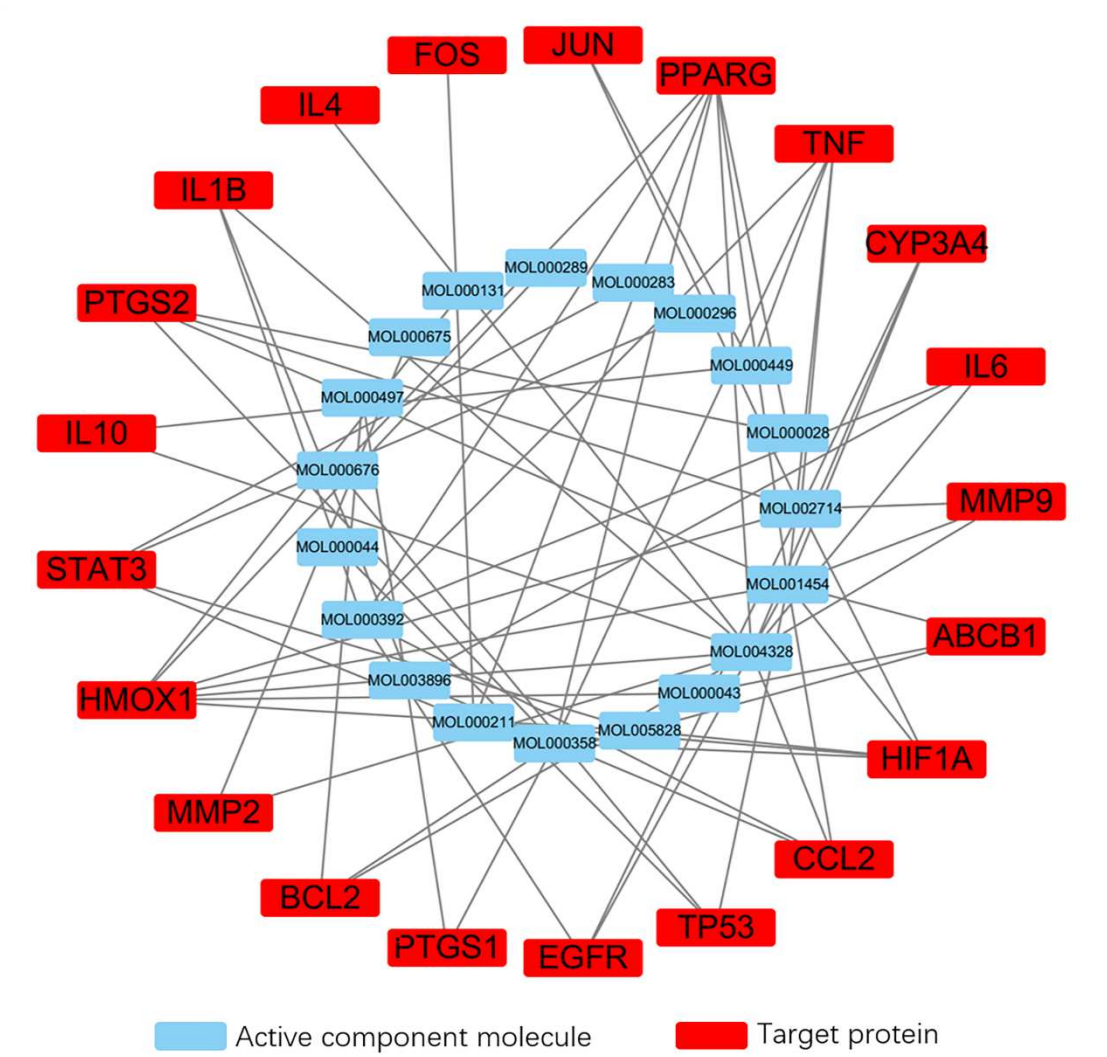

Figure 2: Network diagram of 21 verified targets and their corresponding active components.

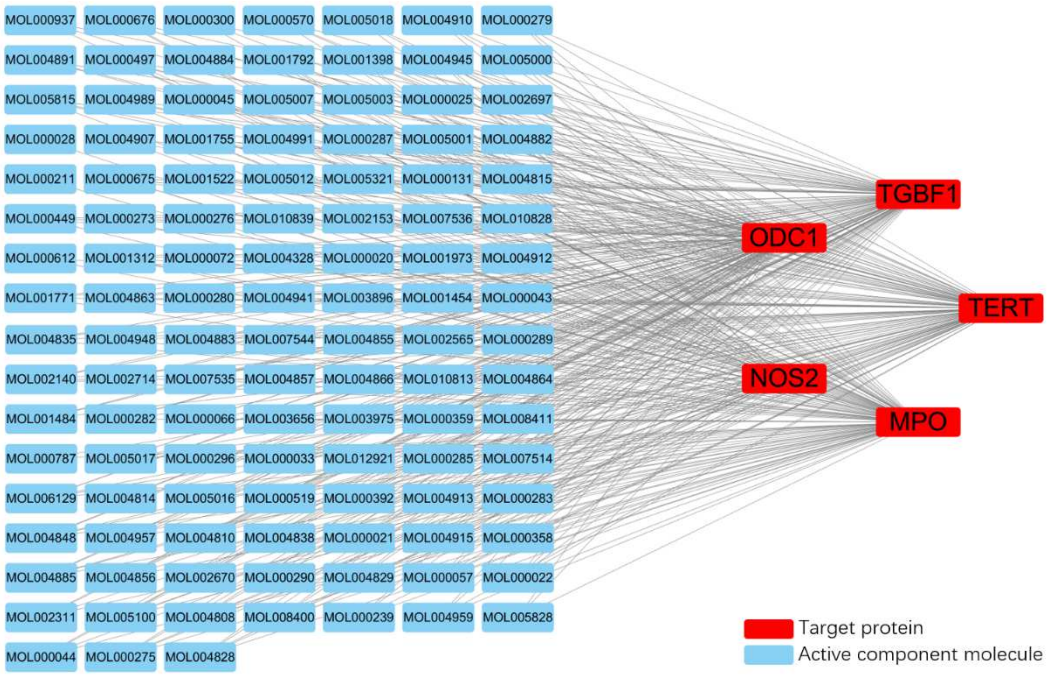

Figure 3: Network diagram of five unverified targets and active component molecules that can be successfully docked with the target in the LibDock mode.

Prediction of the key targets of XSLJP in the treatment of gastritis.

As shown in Figure 4, the protein-protein interaction network (PPI) composed of 26 potential gastritis-related targets (Table 1) of XSLJP contains 26 nodes with 218 edges, and the average node degree value was 16.8. The nodes represent the proteins, and the edges represent the interactions between proteins. A larger node size indicates a greater degree value.

The protein targets interact with each other to achieve therapeutic effects. We performed a topological parameter analysis of these protein targets and identified eight proteins located in the center of the PPI diagram. As shown in Table 2, these eight proteins might be the key targets of XSLJP in the treatment of gastritis.

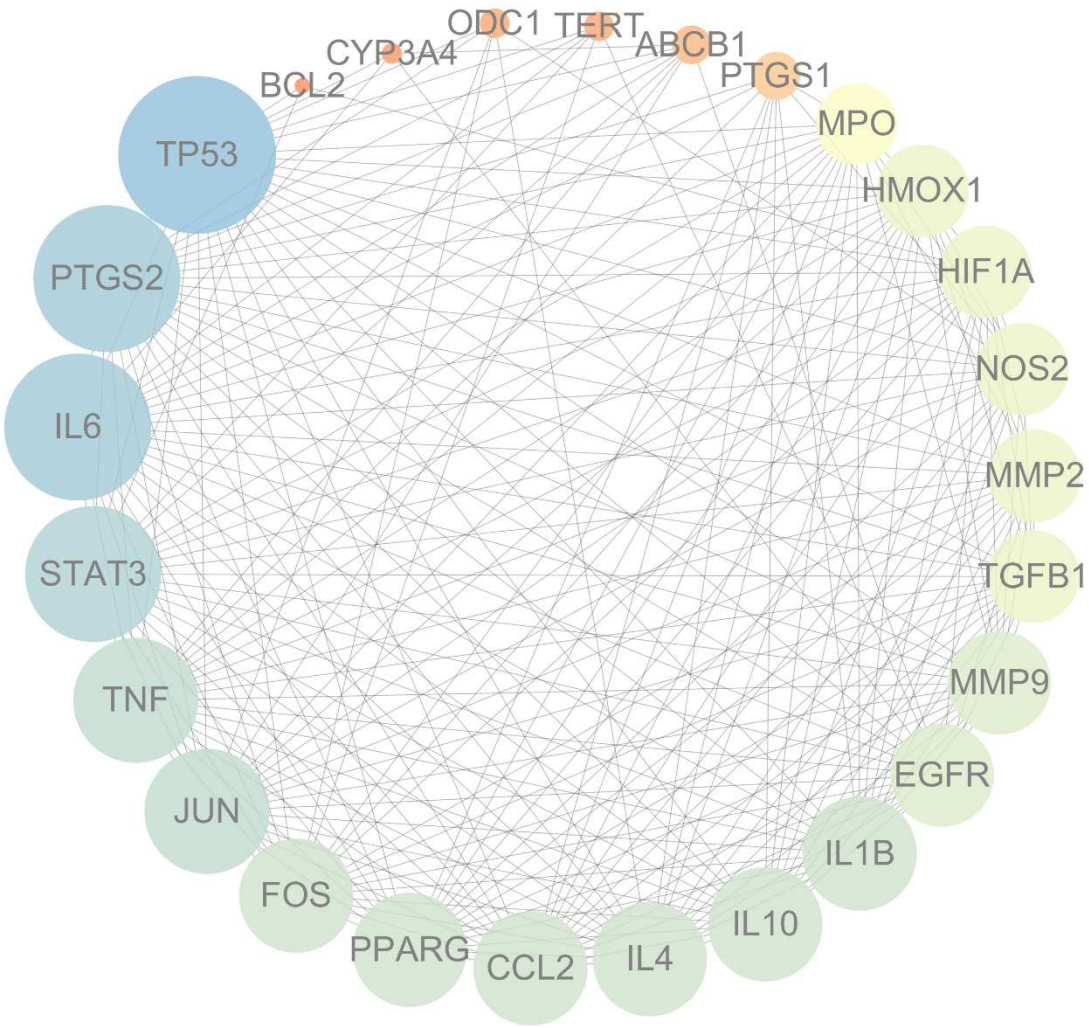

Figure 4: Protein-protein interaction network (PPI) diagram of the 26 common targets.

Table 2: Information on the key targets located in the center of the PPI network.

Gene name	Protein Name	Degree	Betweenness Centrality	Closeness Centrality
TP53	Cellular tumor antigen p53	24	8.25E-02	9.62E-01
IL6	Interleukin-6	23	4.77E-02	9.26E-01
PTGS2	Prostaglandin G/H synthase 2	23	3.53E-02	9.26E-01
STAT3	Signal transducer and activator of transcription 3	22	4.16E-02	8.93E-01

JUN	Jun proto-oncogene	21	1.74E-02	8.62E-01
FOS	Fc fragment of IgG receptor Ⅲb	20	1.77E-02	8.33E-01
EGFR	Epidermal growth factor receptor ErbB1	19	2.73E-02	8.06E-01
HIF1A	Hypoxia-inducible factor 1-alpha	18	1.85E-02	7.81E-01

Prediction of the key active components in XSLJP

The ten TCM herbs (Table 1S), the 118 active components (Table 1S) and the 26 common targets (Table 1) were imported into Cytoscape 3.7.1 software to construct a ‘drug-component-common target’ network diagram that contained 154 nodes and 364 edges, as shown in Figure 5. In this network diagram, the yellow square nodes represent the drugs, the green circular nodes represent the gastritis-related targets, and the remaining square nodes represent the active components. Among the latter nodes, the purple nodes represent the components bound to gastritis-related targets, and the blue nodes represent those that do not bind to gastritis-related targets, as determined by either experimental or computational validation.

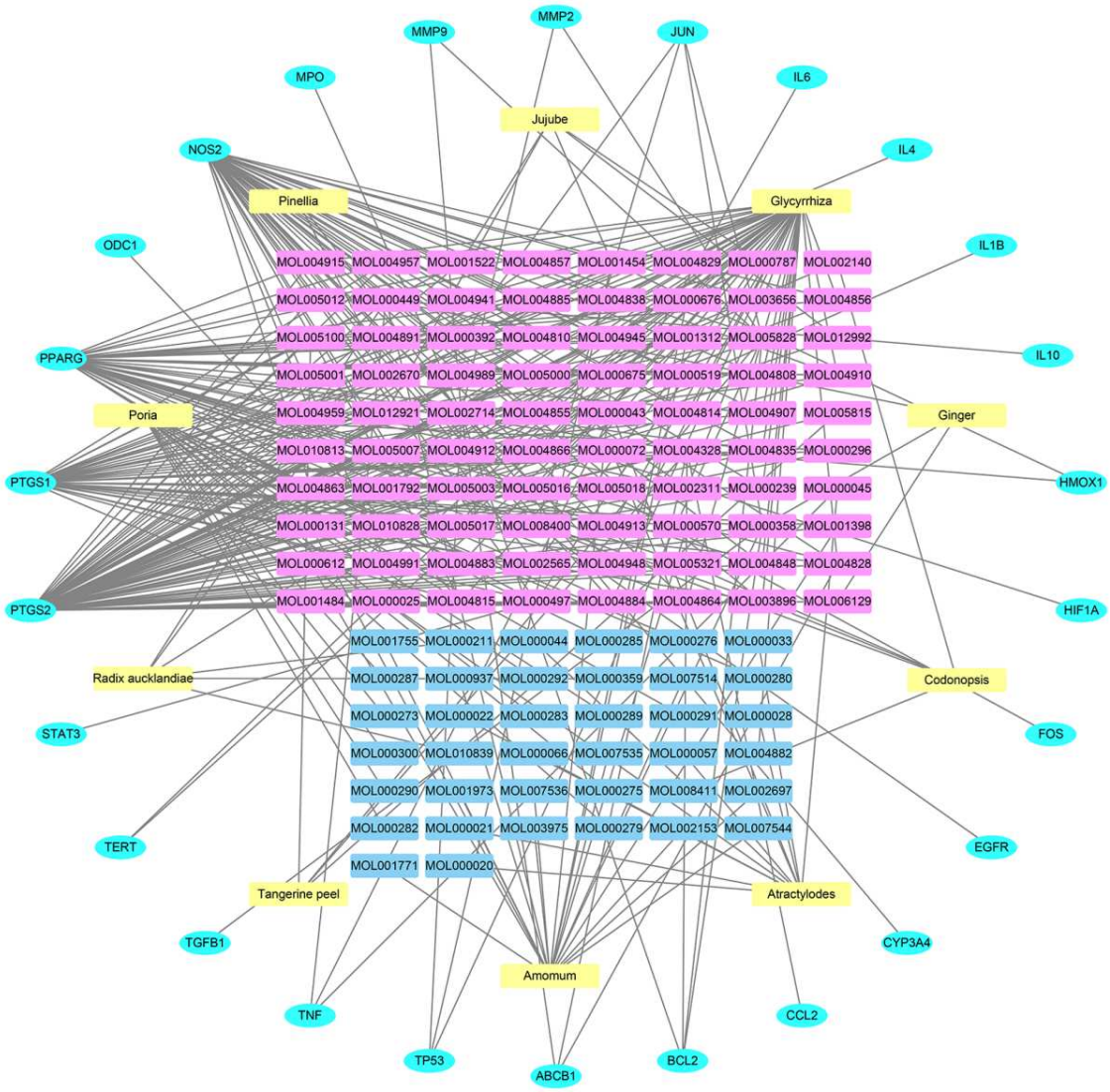

Figure 5: ‘Drug-component-common target’ network diagram.

XSLJP is a complex Chinese herbal medicine with various components, each of which can act on multiple disease targets and play a synergistic role in the treatment of diseases. As intuitively shown in the network diagram (Figure 5), some nodes are more concentrated in the network than others. Therefore, the active components were ranked by degree value, which can be used as the main reference standard in a topological analysis. Using degree > 6 as the threshold, 12 important active components in this prescription were found, which are likely to be the key active components of this prescription in the treatment of this disease. Table 3 shows the

gastritis-related target genes of these 12 active components.

Table 3: Information on the 12 key active components and their corresponding targets.

Mol ID	Degree	Active component	Herb	Target	
				Previously verified	Verified in the current study
MOL002714	12	Baicalein	*PI*	MMP9, HIF1A, EGFR, HMOX1, PTGS2, JUN, TNF, CYP3A4	TERT, ODC1, TGFB1
MOL005828	10	Nobiletin	*TP*	ABCB1, HIF1A, CCL2, HMOX1, STAT3	MPO, ODC1, TGFB1
MOL004328	8	Naringenin	*TP*	MMP9, CCL2, BCL2, MMP2, HMOX1, IL10, IL1B, IL4, PPARG, CYP3A4, IL6	TERT, MPO, ODC1, TGFB1
MOL008400	7	Glycitein	*CO*	/	TERT, NOS2, MPO, TGFB1, ODC1
MOL000449	7	Stigmasterol	*RA/AM/GI*	IL10, JUN, TNF	TERT, MPO, ODC1, TGFB1
MOL000392	7	Formononetin	*GL*	CCL2, EGFR, IL1B, PPARG, TNF, IL6	TERT, MPO, ODC1, TGFB1
MOL000358	7	Beta-Sitosterol	*AM/GI*	HIF1A, PTGS1, BCL2, PTGS2, PPARG, TNF	TERT, MPO, ODC1, TGFB1
MOL004828	6	Glepidotin A	*GL*	/	TERT, NOS2, MPO, TGFB1, ODC1
MOL004815	6	*	*GL*	/	TERT, NOS2, MPO, TGFB1, ODC1
MOL003896	6	#	*CO/GL*	CCL2, IL1B, IL6	TERT, MPO, ODC1
MOL001454	6	Berberine	*JU*	MMP9, ABCB1, HIF1A,CCL2, TP53, EGFR, BCL2, HMOX1, PTGS2, PPARG, TNF, CYP3A4	TERT, MPO, TGFB1, ODC1
MOL000497	6	Licochalcone α	*GL*	PTGS1, BCL2	TERT, MPO, NOS2, ODC1,

TGBF1

Note: *: (E)-1-(2,4-Dihydroxyphenyl)-3-(2,2-dimethylchromen-6-yl)prop-2-en-1-one #: 7-Methoxy-2-methyl isoflavone

Molecular docking of the active components with the key targets

The flexible docking mode in DS software was used to conduct the molecular flexible docking of eight key targets (Table 2) and 12 key active components (Table 3), and the docking results are shown in Table 4. For each key target, the active components with the best flexible docking energies were selected as representatives to show the docking poses: 3D images of these docking poses are shown in Figure 6, and 2D images of the interactions between the eight key targets and their best-docked active components are shown in Figure 7.

Table 4: Docking energies between eight key targets and 12 key active components obtained by flexible docking.

Mol ID	Molecule Name	Flexible Docking Score (Gene Name/PDB ID, -CDOCKER INTERACTION ENERGY)							
		TP53	**IL6**	**PTGS2**	**STAT3**	**JUN**	**FOS**	**EGFR**	**HIF1A**
		6GGA	**1ALU**	**5KIR**	**6NUQ**	**5VPC**	**5VPF**	**3BEL**	**5OP8**
MOL002714	Baicalein	36.0605	31.3986	34.6661	31.9157	35.2962	35.1087	38.0165	41.1303
MOL005828	Nobiletin	41.6575	39.0936	36.8723	37.9533	47.2618	39.4869	41.1759	44.9912
MOL004328	Naringenin	35.9583	39.2056	40.8041	34.5874	42.6349	37.5361	36.5803	41.2761
MOL008400	Glycitein	37.1968	40.2042	69.5127	42.7787	100.947	102.028	50.8868	60.6203
MOL000449	Stigmasterol	36.3805	43.0098	38.6033	34.2369	43.33	34.3709	40.422	50.7195
MOL000392	Formononetin	37.1416	39.8117	61.2005	33.982	80.7786	73.3408	46.0669	52.115

MOL000358	beta-Sitosterol	40.3303	40.3777	47.7691	37.7057	43.26	39.4006	42.4623	49.1203
MOL004828	Glepidotin A	50.7746	64.5126	90.9121	54.0966	92.7171	93.6863	57.3507	66.5643
MOL004815	*	45.5441	38.7195	46.8489	41.4946	44.0769	38.6819	41.3596	50.9278
MOL003896	#	38.1761	29.8178	40.6482	34.2941	38.2972	32.6945	36.6083	38.5724
MOL001454	Berberine	45.5441	42.0403	34.6332	36.1308	37.1438	25.349	45.693	46.7117
MOL000497	Licochalcone α	48.0094	49.7856	54.5744	52.5523	75.8474	70.7379	54.9272	60.7223

Note: *: (E)-1-(2,4-Dihydroxyphenyl)-3-(2,2-dimethylchromen-6-yl)prop-2-en-1-one

#: 7-Methoxy-2-methyl isoflavone

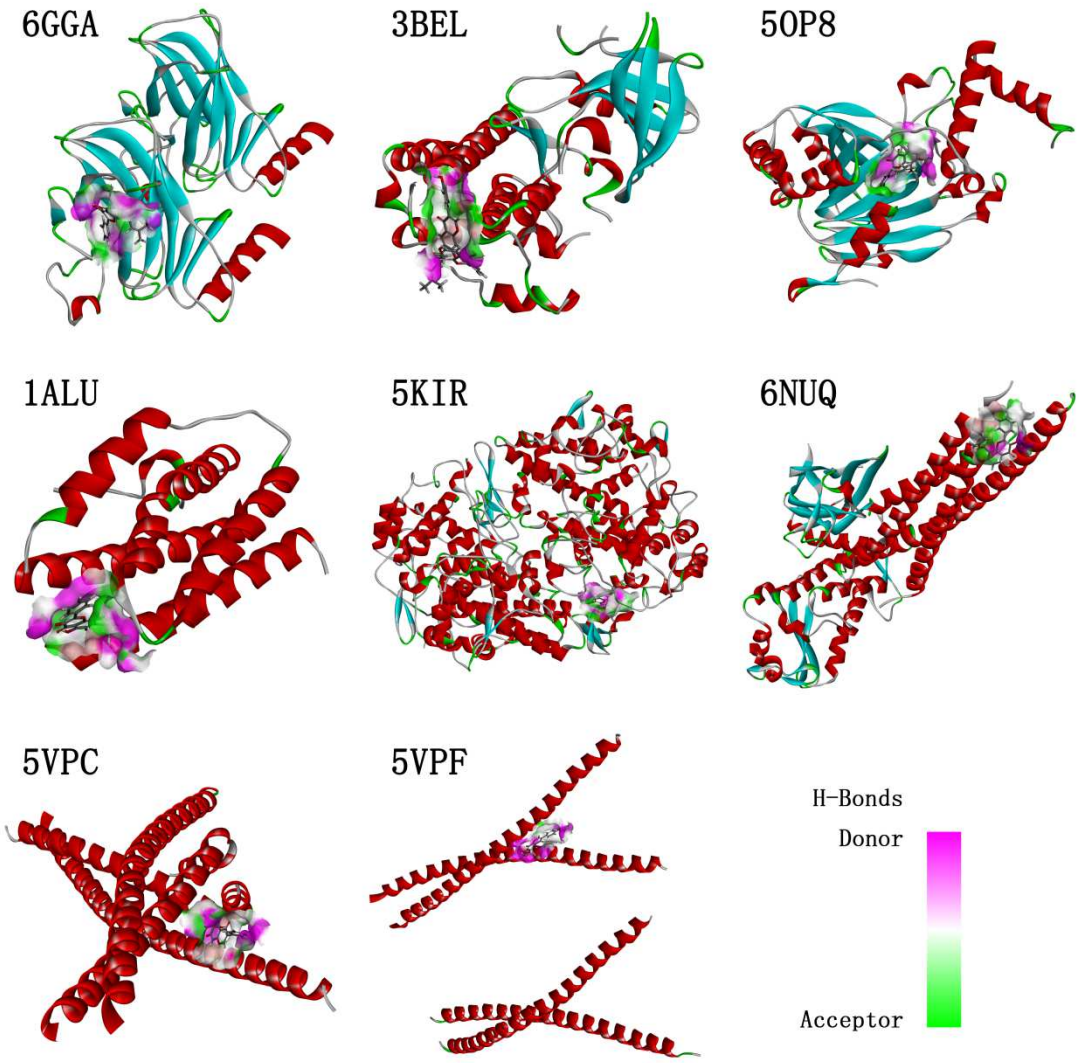

Figure 6: 3D images of the docking poses between the eight key targets and their corresponding active components with the lowest binding energies under the CDOCKER flexible docking model.

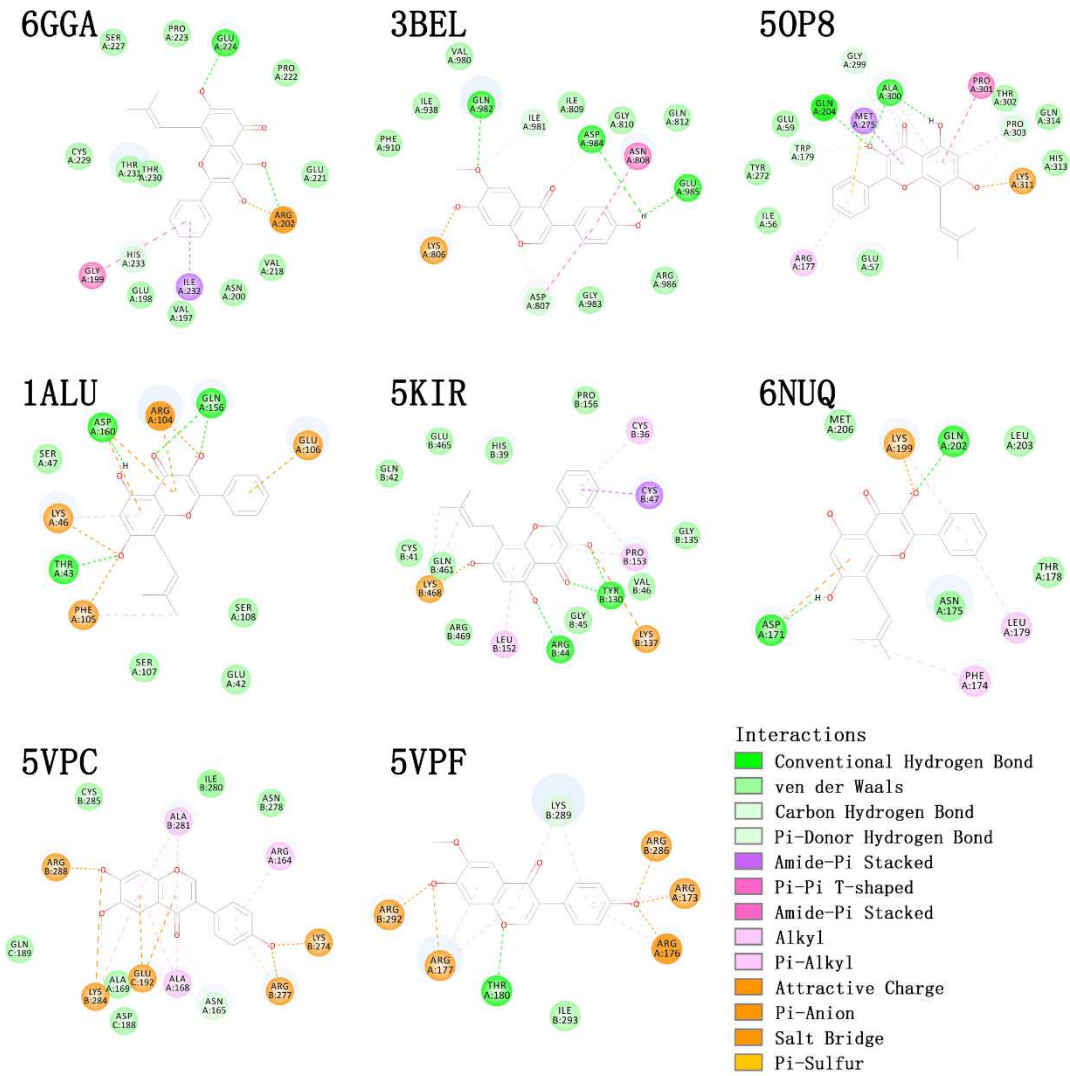

Figure 7: 2D images of the docking poses between the eight key targets and their corresponding active components with the lowest binding energies under the CDOCKER flexible docking model.

Enrichment analysis of the potential targets of XSLJP in the treatment of gastritis

The 26 common targets (Table 1) that might play crucial roles in the treatment of gastritis were imported into the DAVID database for KEGG pathway enrichment analysis and GO biological function analysis with the species set to ‘Homo sapiens’. The analyses yielded 58 KEGG pathways and 230 GO biological processes. Table 5 lists the top 20 KEGG pathways with a *P*-value < 0.05, Figure 8 shows their bubble plot drawn using R language

software, Table 6 lists the top 20 GO biological processes with a *P*-value < 0.05, and Figure 9 shows their bubble plot drawn using R language software.

Table 5: Information on the top 20 pathways identified from the KEGG pathway enrichment analysis.

Term	Count	P-Value	Genes
Pathways in cancer	14	1.58E-10	EGFR, IL6, PTGS2, MMP9, PPARG, TP53, MMP2, STAT3, TGFB1, FOS, HIF1A, JUN, BCL2, NOS2
Leishmaniasis	9	8.08E-11	IL4, FOS, TNF, PTGS2, JUN, IL1B, NOS2, IL10, TGFB1
Chagas disease (American trypanosomiasis)	9	1.82E-09	FOS, IL6, TNF, CCL2, JUN, IL1B, NOS2, IL10, TGFB1
Hepatitis B	9	2.57E-08	FOS, IL6, TNF, JUN, BCL2, MMP9, TP53, TGFB1, STAT3
Inflammatory bowel disease (IBD)	8	1.82E-09	IL4, IL6, TNF, JUN, IL1B, IL10, TGFB1, STAT3
TNF signaling pathway	8	6.90E-08	FOS, IL6, TNF, CCL2, PTGS2, JUN, MMP9, IL1B
Proteoglycans in cancer	8	4.87E-06	EGFR, TNF, HIF1A, MMP9, TP53, MMP2, TGFB1, STAT3
MicroRNAs in cancer	8	5.03E-05	EGFR, PTGS2, HMOX1, BCL2, MMP9, TP53, ABCB1, STAT3
Pertussis	7	2.06E-07	FOS, IL6, TNF, JUN, IL1B, NOS2, IL10
Rheumatoid arthritis	7	5.38E-07	FOS, IL6, TNF, CCL2, JUN, IL1B, TGFB1
HIF-1 signaling pathway	7	9.02E-07	EGFR, IL6, HIF1A, HMOX1, BCL2, NOS2, STAT3
Tuberculosis	7	3.14E-05	IL6, TNF, BCL2, IL1B, NOS2, IL10, TGFB1
Herpes simplex infection	7	3.79E-05	FOS, IL6, TNF, CCL2, JUN, TP53, IL1B
Cytokine-cytokine receptor interaction	7	1.84E-04	IL4, IL6, TNF, CCL2, IL1B, IL10, TGFB1
MAPK signaling pathway	7	2.29E-04	EGFR, FOS, TNF, JUN, TP53, IL1B, TGFB1

HTLV-I infection	7	2.34E-04	FOS, IL6, TNF, JUN, TP53, TGFB1, TERT
Malaria	6	7.10E-07	IL6, TNF, CCL2, IL1B, IL10, TGFB1
Amoebiasis	6	3.29E-05	IL6, TNF, IL1B, NOS2, IL10, TGFB1
Toxoplasmosis	6	3.93E-05	TNF, BCL2, NOS2, IL10, TGFB1, STAT3
Osteoclast differentiation	6	9.08E-05	FOS, TNF, JUN, PPARG, IL1B, TGFB1

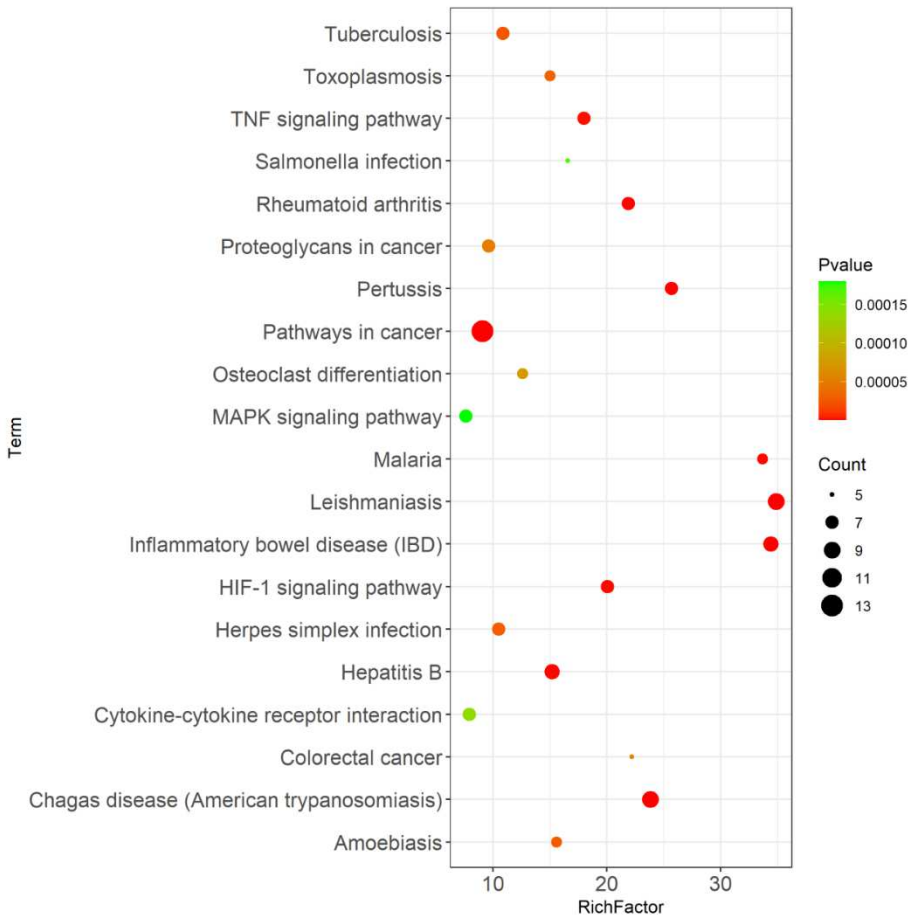

Figure 8: Bubble plot of the top 20 pathways obtained from the KEGG enrichment analysis.

As shown in Figure 8, 26 targets of XSLJP in the treatment of gastritis were predominant in various pathways, including infectious disease pathways, immune inflammatory pathways, cancer pathways, signaling pathway, and cell growth and death pathways. The top 20 KEGG pathways included nine infectious disease pathways, namely, leishmaniasis, Chagas diseases, pertussis, malaria, tuberculosis, amoebiasis, herpes simplex infection, toxoplasmosis and hepatitis B; three immune inflammatory pathway, namely, inflammatory bowel disease, rheumatoid arthritis and HTLV-I infection; three cancer pathways, namely, pathways in cancer, proteoglycans in cancer and microRNAs in cancer; three cell growth and death pathways, namely, the TNF signaling pathway, osteoclast differentiation and cytokine-cytokine receptor interaction; and two signaling pathways, namely, the HIF-1 signaling pathway and the MAPK signaling pathway. The pathway with the smallest P-value of 8.08E-11 was leishmaniasis, whereas that with the largest count of 14 was pathways in cancer.

Table 6: Information on the top 20 biological processes identified from the GO functional enrichment analysis.

Term	Count	P-value	Genes
Positive regulation of transcription from RNA polymerase II promoter	13	3.79E-09	IL4, EGFR, IL6, TNF, PPARG, TP53, STAT3, TGFB1, IL10, FOS, HIF1A, JUN, IL1B
Positive regulation of transcription, DNA-templated	12	6.14E-11	IL4, FOS, IL6, TNF, HIF1A, JUN, PPARG, TP53, IL1B, IL10, TGFB1, STAT3
Response to drug	11	8.39E-12	IL4, FOS, IL6, PTGS2, JUN, BCL2, PPARG, ABCB1, IL10, TGFB1, STAT3
Inflammatory response	9	4.84E-08	FOS, IL6, TNF, CCL2, PTGS2, PTGS1, IL1B, IL10, TGFB1
Negative regulation of apoptotic process	9	1.97E-07	IL4, EGFR, IL6, BCL2, MMP9, TP53, MPO, IL10, STAT3
Aging	8	3.22E-09	FOS, IL6, CCL2, JUN, MPO, IL10, TGFB1, STAT3
Negative regulation of cell proliferation	8	1.28E-06	IL6, PTGS2, JUN, TP53, IL1B, IL10, TGFB1, STAT3

Positive regulation of gene expression	7	1.88E-06	IL6, TNF, HIF1A, TP53, IL1B, TGFB1, STAT3
Positive regulation of pri-miRNA transcription from RNA polymerase II promoter	6	7.30E-11	FOS, HIF1A, JUN, TGFB1, TERT, STAT3
Positive regulation of smooth muscle cell proliferation	6	2.47E-08	EGFR, IL6, TNF, PTGS2, JUN, HMOX1
Cellular response to hypoxia	6	2.67E-07	HIF1A, PTGS2, HMOX1, BCL2, TP53, TERT
Positive regulation of sequence-specific DNA-binding transcription factor activity	6	4.18E-07	IL4, IL6, TNF, PPARG, IL1B, IL10
Response to hypoxia	6	4.79E-06	HIF1A, CCL2, HMOX1, NOS2, MMP2, TGFB1
Positive regulation of ERK1 and ERK2 cascade	6	5.21E-06	EGFR, IL6, TNF, CCL2, JUN, TGFB1
Angiogenesis	6	1.69E-05	HIF1A, CCL2, PTGS2, JUN, HMOX1, MMP2
Positive regulation of apoptotic process	6	6.97E-05	IL6, TNF, PTGS2, HMOX1, TP53, TGFB1
Immune response	6	3.40E-04	IL4, IL6, TNF, CCL2, IL1B, IL10
Positive regulation of cell proliferation	6	5.41E-04	EGFR, ODC1, IL6, BCL2, TGFB1, STAT3
Negative regulation of transcription, DNA-templated	6	7.37E-04	IL4, TNF, JUN, PPARG, TP53, TGFB1
Signal transduction	6	2.61E-02	EGFR, HIF1A, CCL2, PPARG, IL1B, STAT3

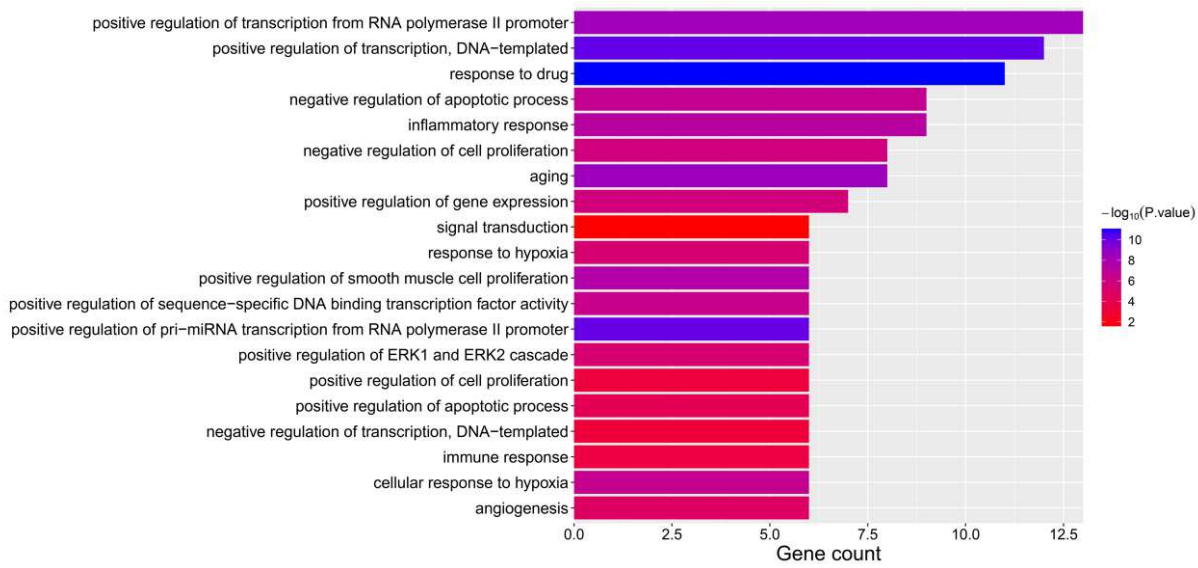

Figure 9: Bar plot of the top 20 biological processes obtained from the GO biological function analysis.

As shown in Figure 9, the gastritis-related targets are involved in a variety of biological processes, which mainly include the biological processes that regulate reactions, growth/apoptosis and gene expression. The top 20 biological processes include eight biological processes that regulate growth and apoptosis, namely, positive regulation of cell effort, positive regulation of smooth muscle cell effort, negative regulation of cell effort, aging, angiogenesis, signal transduction, positive regulation of apoptotic process, negative regulation of apoptotic process; seven biological processes that regulate gene expression, namely, positive regulation of transcription (DNA-templated), positive regulation of transcription from RNA polymerase II promoter, transcription of pri-miRNA transcription from RNA polymerase II promoter, positive regulation of link-specific DNA binding transcription factor activity, positive regulation of ERK1 and ERK2 cascade, and negative regulation of transcription (DNA-templated); and five biological processes that regulate reactions, namely, response to drug, response to hypoxia, cellular response to hypoxia, immune response, and inhibitory response. In addition, the biological process with the smallest P-value of 8.39E-12 was response to drug, whereas that with the largest count of 13 was positive regulation of transcription from RNA polymerase II promoter.

Discussion

Gastritis, a general digestive system disease resulting from a variety of factors, is a type of infectious or autoimmune inflammation characterized by gastric mucosal damage [30]. At present, the first-line drugs for gastritis therapy are antibiotics and proton pump inhibitors, but these drugs are not sufficiently specific to this disease and have serious side effects [31, 32]. In addition, the nonsteroidal anti-inflammatory drugs (NSAIDs) commonly used in the clinic to reduce inflammation can easily cause gastric mucosal damage and subsequently induce peptic ulcers [33]. Significantly, long-term chronic inflammation of the gastric mucosa might lead to atrophy of the mucosa and glands and could even develop into gastric cancer [34]. Therefore, it is necessary to find safer and more effective drugs from natural drugs for the treatment of gastritis. TCM prescriptions have gradually developed through the processing of compatible Chinese herbal medicines according to long-term and rich experiences. TCMs are characterized by the synergistic effect of multiple components, and their advantages lie in long-lasting efficacy, mild medicinal properties, nourishing effects, and outstanding effects on the treatment of chronic diseases [35]. XSLJP is a complex TCM prescription with a complicated mechanism that remains unelucidated. Clearly exploring the mechanism of XSLJP and reasonably adjusting the drug dosage according to the drug characteristics will improve the application of XSLJP in the clinical treatment of gastritis.

Active components and corresponding targets of XSLJP in the treatment of gastritis

In this study, 26 potential targets of XSLJP in the treatment of gastritis were identified (Table 1), and 21 of these were verified by literature mining using the PubMed database, which demonstrated the reliability and validity of this study. In addition, molecular docking simulations demonstrated that the remaining five targets can be well docked with some of the active components of XSLJP (Table 5S and Figure 3), which suggests that the 26 key targets are likely the main targets of XSLJP in the treatment of gastritis. Subsequently, we analyzed the topological parameters of these 26 targets according to their PPI diagram (Figure 4) and obtained eight targets with a high degree of interaction (Table 2), and these eight targets, namely, TP53, IL6, PTGS2, STAT3, JUN, FOS, EGFR, and HIF1A, might be the key targets

of XSLJP in the treatment of gastritis.

To date, most of the active components of XSLJP have been confirmed to have biological activity and various pharmacological effects. The interactions between different active components in a TCM preparation exert a therapeutic effect as a whole, and the preparation must have certain key active components that exert the major pharmacological effects. According to the ‘drug-compound-common target’ network (Figure 5), we identified 12 potential key active components of XSLJP with a degree higher than 6 (Table 3). The targets related to these 12 key active components are consistent with 24 of the 26 potential targets of XSLJP in the treatment of gastritis (Table 1), which demonstrates that these 12 key active components are likely the key active components of XSLJP in the treatment of gastritis.

Based on the abovementioned identifications, flexible docking simulations between the 12 key active components and the eight key targets were conducted to further explore their mode of interactions. The results showed that all 12 key active components and eight key targets had good docking scores (Table 4) with satisfactory docking postures (Figure 6 and Figure 7). Moreover, according to the docking score results, a heatmap was drawn to show the correlation between the key components and key targets (Figure 10). As shown in the figure, four key active components, namely, glycitein, formononetin, glepidotin A and licochalcone α, had relatively better docking scores with most of the eight hub targets. These findings are particularly interesting because they provide novel ideas as described below for further studies of this TCM medicine, including biological experimental verification, XSLIP prescription adjustment and single-component Western medicine development.

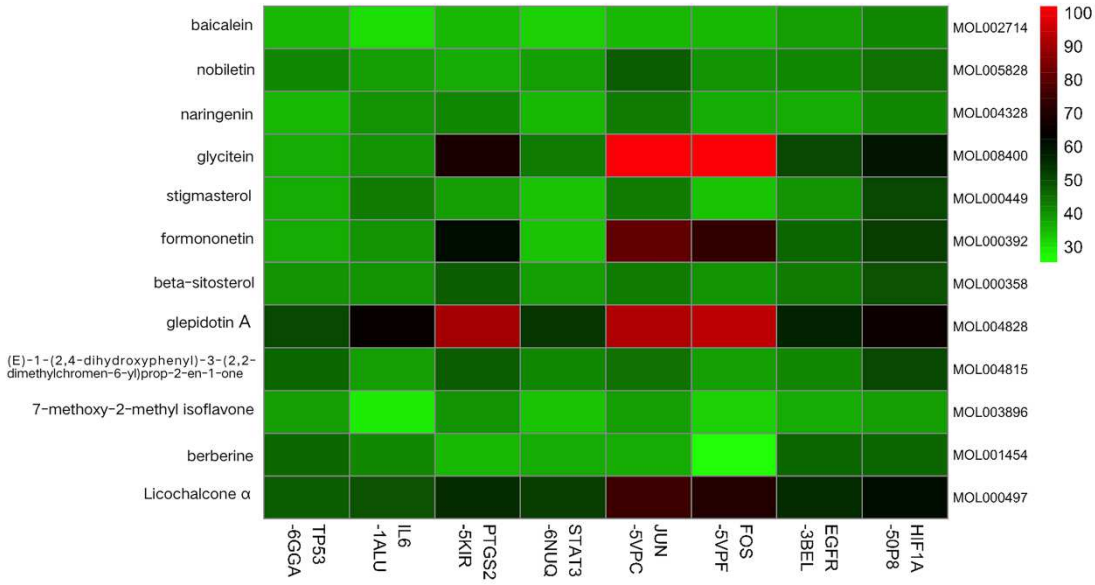

Figure 10: Heatmap displaying the docking scores between the 12 key components and eight hub targets.

Potential key signaling pathways involved in the mechanisms of XSLJP in the treatment of gastritis

In our study, the GO biological function analysis (Table 6 and Figure 9) showed that the abovementioned targets are related to a variety of biological processes, including positive regulation of transcription from the RNA polymerase II promoter and positive regulation of transcription. In addition, the KEGG enrichment analysis (Table 5 and Figure 8) revealed that these targets are involved in infectious disease pathways and immune inflammatory pathways, among other pathways. These results indicate that the mechanism of XSLJP in the treatment of gastritis might be related to these extensive and intricate signaling pathways.

Figure 11 shows a schematic diagram of the possible mechanism of XSLJP based on the 26 common targets and their main enriched signals. In the figure, the boxes represent the corresponding proteins encoded by the gene targets, and the green and yellow boxes represent the experimentally verified targets and the key targets, respectively. The schematic diagram shows the positions of the proteins encoded by the 26 genes in the signal pathways and their upstream and downstream relationships. On the one

hand, Figure 11 shows the existence of several target clusters, and these are mainly concentrated in the TNF, JAK/STAT, MAPK (ERK/JNK/p38), p53 and NO/VEGF signaling pathways. On the other hand, most of the predicted targets of the active components are closely related to immune regulation and influence various inflammatory cytokines, including IL-1β, IL-6/8/10/12, TNF-α, COX-2, iNOS, NO, TGF-β, NF-κB, and IFN-γ, to regulate the immune process of the body. The following discussion will focus on the key active components, the key targets and their corresponding signaling pathways related to XSLJP in the treatment of gastritis.

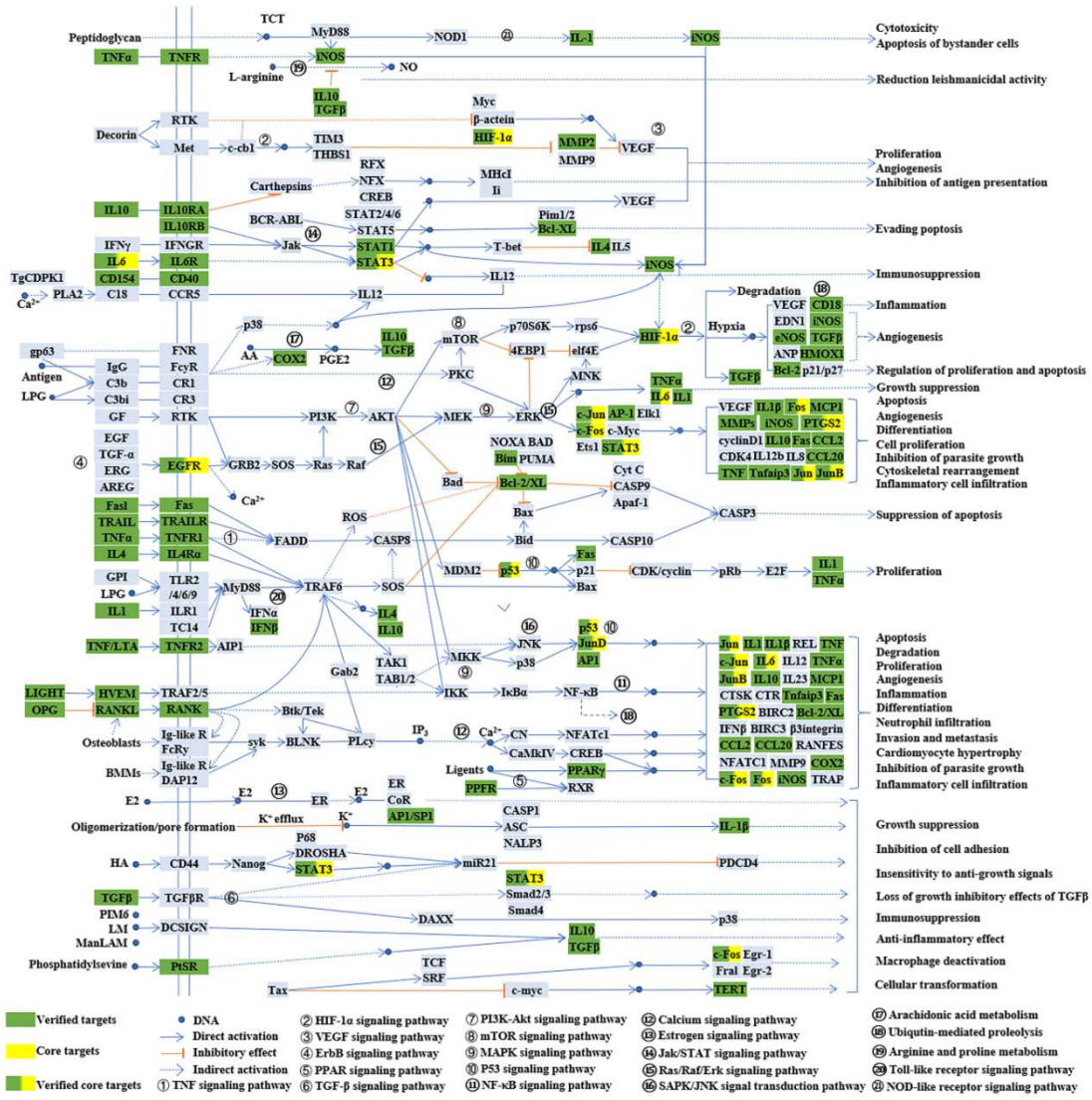

Figure 11: Complete signaling pathways identified from the exploration of

the potential mechanism of XSLJP in the treatment of gastritis.

XSLJP and the TNF signaling pathway

Figure 1S shows detailed information on the TNF signaling pathway. TNF-α can be regulated by some gene promoters, such as NF-κB, c-Jun, and AP1, and subsequently induces apoptosis by TNF-α family proteins, such as FasL, TNF-α and TRAIL, whose expression is mediated by linker proteins containing death domains, such as FADD [36]. By mediating linker proteins without the death domain, such as TRAF, TNF-α can induce Toll-like receptor (TLR), IL-1 receptor (IL1R) or other members of the TNF family to activate NF-κB, JNK, p38 and other downstream signaling pathways [36]. Due to its pivotal location with respect to the TLR downstream signaling pathway, NF-κB can induce chemotactic granulocytes and macrophages, increase capillary permeability and cause lymphocyte infiltration to participate in the early immune response and inflammatory reaction by initiating target genes to express inflammatory factors, such as TNF-α, IL-1/6/8/12 and IFN [37]. The activation of this pathway can not only directly stimulate the synthesis of ICAF and IL-1 to promote cell adhesion, proliferation and inflammation but also indirectly stimulate other cells to produce vascular growth factor and promote angiogenesis and the apoptosis of transformed cells [38]. Formononetin, naringenin, berberine and other active components of XSLJP can regulate the expression of TNF, IL-1B, IL-10 and other cytokines in the TNF signaling pathway. For instance, formononetin can reduce intracellular calcium, restrict the activation of NF-κB, the phosphorylation of its upstream protein IκKα and the activity of caspase-1, and further inhibit the release of histamine and the secretion of TNF-α, IL-1β and IL-6, which ultimately results in the exertion of antioxidant, anti-inflammatory, proapoptotic and antitumor activities [39]. Naringenin can reduce the lung injury of mice with mycoplasma pneumonia to exhibit anti-inflammatory activity by inhibiting the expression of autophagy-mediated proinflammatory cytokines, such as IL-6, IL-1β, TNF-α and TGF-β, as well as pulmonary fibrosis [36]. Berberine can significantly inhibit the expression of IL-6 and TNF-α in human HK-2 cells damaged by palmitic acid (PA) and can attenuate PA-induced lipotoxicity through the PPAR-α pathway [40]. In addition, our calculations revealed that glepidotin A showed the best docking to IL-6 with the lowest docking energy, which suggests that glepidotin A might exert a series of downstream biological effects by binding with the IL-6 protein to mediate its protein expression

level and biological function, but this hypothesis needs to be verified by future experiments. It is worth noting that glepidotin A can also combine tightly with all seven other hub targets, particularly PTGS2, JUN and FOS, with very low docking energies, which implies that this compound might significantly contribute to pill therapy for gastritis and has the potential to be developed into a single component-multiple target agent.

XSLJP and the JAK/STAT signaling pathway

Figure 2S shows detailed information on the JAK/STAT signaling pathway. Cytokines such as STAT3, CCL2, IFN-α/β/γ, IL-6/10 and MMP-9 can activate the JAK/STAT signaling pathway in host cells [41]. These cytokines can phosphorylate JAK to activate STAT3, which can enter the cell nucleus and further combine with its target gene promoters to stimulate transcription [41]. STAT3 protein plays an important role in selectively inducing and maintaining the oncogenic inflammatory microenvironment at the beginning of malignant transformation and cancer development [42]. In addition, activated JAKs can also upregulate the expression of STAT3 via the Grb2/mTOR or Grb2/Ras/Raf/MEK/p-ERK/TF pathways [43]. As a crucial activator of STAT3 [44], IL-6 can indirectly promote the production of the proinflammatory factor CCL2 in monocytes to drive downstream Ca^{2+} signal transduction and thereby lead to enhanced expression of MMP-9, which can degrade a variety of extracellular matrix components and further promote tumor cell infiltration and metastasis [45]. In addition, CCL2 can trigger the secretion of CCL2/CCR2 to promote and maintain the generation of an immunosuppressive microenvironment [45]. IL-10, a major immunomodulatory cytokine, can activate STAT3 phosphorylation directly in a positive feedback manner due to the STAT3 binding site in its promoter after JAK activation [45, 46]. IL-10 can also downregulate the production of IL-12 and the expression of costimulatory molecules in macrophages and thereby reduces the generation of the Th1 response [47]. Ergosterol peroxide (EP), nobiletin, naringenin and other active components of XSLJP can affect the expression of cytokines in the JAK/STAT signaling pathway, such as STAT3, CCL2, IFN-α/β/γ, IL-6/10 and MMP-9. For instance, EP can significantly inhibit the phosphorylation of STAT3 and the expression and secretion of VEGF-C, and as a result, EP can counteract tumor angiogenesis and thereby suppress ovarian tumor growth[48]. Similarly, by reducing the activity and expression of STAT3, nobiletin can inhibit the angiogenesis of CD36-dependent breast cancer cells [49] and estrogen receptor-positive

(ER^+) breast cancer cells [50]. In addition, nobiletin can significantly and dose-dependently inhibit the secretion of inflammatory mediators such as NO, TNF-α and CCL2 in a coculture of adipocytes and macrophages [51]. Another active component, naringenin, can upregulate the expression of IL-6/10/18R1/18RAP, MMP-2/-3/-9, IFG1R and BCL2 and thus exerts anti-inflammatory and regenerative effects in degenerated human NP cells [52]. As demonstrated by our calculations, licochalcone α, in addition to glepidotin A as described above, exhibits high binding affinity to the active pocket of STAT3, which pending experimental verification, suggests that licochalcone α might combine with STAT3 and inhibit the expression of STAT3 or the biological effects of STAT3 against gastritis.

XSLJP and the MAPK (ERK/JNK/p38) signaling pathway

Figure 3S shows detailed information on the MAPK (ERK/JNK/p38) signaling pathway. Activation of the ERK1/2 pathway mainly amplifies the signal, whereas activation of the p38 pathway induces the expression of IL-1β/6/8, TNF-α, COX-2, iNOS, and prostaglandins, which participate in the proliferation and differentiation of immune cells [53, 54]. In the JNK/SAPK pathway, JNK can be activated by cytokines such as VEGF, IFN-α, IL-1, TRAF2, TGF-β and TNF-α and can then be phosphorylated and incorporated into the nucleus through the MAPK cascade reaction to act on downstream transcription factors such as c-Jun, c-Fos, AP-1, Elk1, p53, c-Myc, and Smad4 [53-55]. In the presence of IL-6, TGFβ1 drives the differentiation of T helper 17 (Th17) cells and then promotes further inflammation and enhances autoimmune conditions [56]. After binding to epidermal growth factor (EGF) and other ligands, EGFR autophosphorylates and stimulates Ras protein, which triggers gene transcription and control cell proliferation, differentiation and survival by activating signaling pathways such as the MAPK and PI3K/Akt pathways [57]. When the gastric mucosa is injured, the expression of EGFR in gastric parietal cells and related tissues is significantly increased [58], which might enhance the expression or activity of EGFR downstream signaling molecules such as ERK2, MEK1, AP1 and plasma membrane RTK [57]. In addition, EGFR can activate STAT3 and induce a series of biological effects downstream of STAT3, as discussed above discussion. Berberine, formononetin, and other active components of XSLJP can affect the expression of TGFB1, IL-6, TNF, EGFR and other cytokines in the MAPK signaling pathway. For instance, berberine can greatly reduce the expression of EGFR, further inhibit the phosphorylation

of Raf, MEK and ERK, and thereby induce glioblastoma senescence [59]. Formononetin, another key component, has been identified as an EGFR inhibitor that can inhibit the tumor growth of nonsmall cell lung cancer through the EGFR/Akt/Mcl-1 pathway [60]. In this study, naringenin was the best-docked compound to TGFB1 in the LibDock mode (Table 5S), which suggests that this compound might directly bind to TGFB1, but its induction of the expression of TGFB1 and further downstream effects on gastritis need to be verified by biological experiments. In addition, glycitein exhibited significant binding affinity within the active site of EGFR, c-Jun and c-Fos, which suggests that glycitein might also target these three proteins to inhibit the expression of EGFR and the downstream transcription factors c-Jun and c-Fos or influence its downstream biological effects in gastritis therapy, but these effects remain to be confirmed by further experiments.

XSLJP and the p53 signaling pathway

Figure 4S shows detailed information on the p53 signaling pathway. As a key node in the p53 signaling pathway, p53, a transcription factor, can interact with a variety of functional proteins to induce a series of biological effects, such as blocking the cell cycle, promoting apoptosis, repairing DNA and inhibiting tumor angiogenesis and inflammation [61]. As an important downstream protein of p53 and a cyclin-dependent protein kinase inhibitor, p21 can bind to a series of cyclin-CDK complexes to inhibit the activity of corresponding protein kinases and thereby affects the phosphorylation of its downstream protein, interferes with the transcriptional regulation of CDK/cyclin complexes and ultimately causes cell cycle arrest [62, 63]. Moreover, the p53 protein triggers cell apoptosis unless it applies its own exonuclease activity to repair damaged DNA by forming a complex with p21 and GADD45 [64]. Under most conditions, regulated by the p53 protein concurrently with the apoptotic protein Bax, Bcl-2 exerts an anti-apoptotic effect by preventing the release of apoptosis-forming factors such as cytochrome C from the mitochondria, regulating the transcription factors NF-κB, AP-1, CRE and NFAT by blocking their entry into the nucleus, and thereby jointly promoting apoptosis [65]. Di-n-butyl phthalate, atractylenolide II, naringenin, berberine and other active components of XSLJP can affect the expression of p53, Bcl-2, and other cytokines in the p53 signaling pathway. For instance, di-n-butyl phthalate can effectively induce the apoptosis of mouse osteoblasts through the downstream effect

mediated by p53 activation [66]. Atractylenolide II can decrease the expression of CDK2, p-AKT, p-ERK and Bcl-2, increase the phosphorylation of p38 and p53, p21 and p27, and further activate caspase-3/-8/-9, which results in the induction of G1 cell cycle arrest and apoptosis in B16 melanoma cells [67]. Naringenin can upregulate the expression of IL6/10, MMP-2/-3/-9 and Bcl-2 and downregulate the expression of IL1A and CASP3 in degenerated human nucleus pulposus cells, and thus, this compound exhibits anti-inflammatory and regenerative effects [52]. Berberine can trigger the release of cytochrome C from the mitochondrial membrane space into the cytoplasm, significantly increase the expression of caspase-3/-7/-9, cleaved PARP and Bax and reduce that of Bcl-2, which ultimately results in activation of the apoptotic pathway [68]. Among the key predicted components identified in this study, berberine exhibited low binding energies with TP53, which suggests that berberine might affect a series of downstream biological effects by binding to the p53 protein to induce apoptosis in gastritis cells, but this hypothesis needs to be verified by further experiments.

XSLJP and the NO/VEGF signaling pathway

Figure 5S shows detailed information on the NO/VEGF signaling pathway. COX-1 encoded by the PTGS1 gene mainly exists in normal tissue cells and is responsible for the production of endogenous prostaglandins (PGs) involved in mucosal protection, whereas COX-2 encoded by the PTGS2 gene is generally expressed in inflammatory environments and cancer tissues rather than normal tissues [69]. In most cases of inflammation and cancer, COX-2 and NF-κB are often activated simultaneously, whereas inactivated EGFR triggers the EGFR signaling pathway through negative feedback to promote cancer cell proliferation [70]. Inflammatory factors such as NF-κB, IL-6/-8, and IFN-γ exert a certain therapeutic effect on gastric ulcers by stimulating inflammatory cells to express iNOS and produce NO, and the enhancement of this compounds might promote the protection of mucosal glycoproteins and reduce oxidative stress, which is speculated to be the therapeutic mechanism for gastric ulcers [71]. Under hypoxic conditions, an increase in HIF-1, a cell hypoxia receptor molecule encoded by the HIF1A gene, can stimulate the activation of VEGF, a basic factor for vascular growth regulation, and stimulate angiogenesis to promote oxygen delivery [72]. Berberine, mairin, nobiletin, licochalcone α, and other active components of XSLJP can affect the

expression of COX-1/2 and iNOS in the NO/VEGF signaling pathway. For instance, berberine can downregulate the expression of HIF-1α and VEGF, inhibit the phosphorylation of Akt and ERK, and suppress the growth of NSCLC cells through main pathways, such as NF-κB/COX-2, HIF-1α/VEGF, PI3K/Akt, and RAR/MEK/ERK [68]. Mairin can inhibit the expression and transcriptional activity of HIF-1α under hypoxic conditions, inhibit the nuclear accumulation of STAT3 and the expression of key factors such as VEGF, and protect against angiogenesis in hypoxic PC-3 prostate cells [73]. Nobiletin can reduce the expression of NF-κB and HIF-1α and the phosphorylation of Akt in both PC-3 and DU-145 cells and further downregulate the expression of VEGF and c-Myc respectively to suppress the viability of these two cell lines [74]. Licochalcone α exerts a strong inhibitory effect on the production of thromboxane A2, arachidonic acid and collagen-induced platelet aggregation and thereby inhibits the expression of COX-1 and COX-2 against inflammation [75]. Among the key predicted components identified in this study, formononetin showed good binding affinity to both PTGS2, Jun and HIF1A, which suggests that formononetin is likely to integrate with these proteins to affect their expression level or induce their downstream function in suppressing the inflammatory process in gastritis. However, the existence of a direct interaction between this active component and its target proteins remains to be further verified by experiments.

The pharmacological effects of active components in TCM prescriptions are complementary to each other. As shown in Figure 2 and Figure 3, the following finding was obtained for all the targets, regardless of their experimental verification: either one active component corresponds to multiple targets or multiple components act on the same target, which indicates that the TCM prescription XSLJP treats gastritis through a multitarget and multichannel approach. Attentionally, the signaling pathways mainly included the TNF, JAK/STAT, MAPK, p53 and NO/VEGF signaling pathways, and the regulation of some active compounds on these pathways had been verified, which indicates the scientificity and reliability of this study. Notably, this study showed that the core active ingredients glepidotin A, licochalcone α, glycitein, berberine and formononetin interact with most of the core targets at the optimal level, which implies the importance of these core active ingredients in gastritis therapy, but the interaction between these compounds and core targets requires experimental verification. As indicated by the discussion above, this

research has the potential to provide basic ideas for and guide follow-up studies on the mechanism of XSLJP in the treatment of gastritis.

Outlook/Prospects

In addition to exploring the mechanism of XSLJP in the treatment of gastritis, our research can also provide certain reference ideas for the future optimization of prescription compositions, dosage adjustment, clinical applications and the adjustment of combination schemes. For example, lauric acid, an active component in *Codonopsis*, possesses antibacterial, anti-inflammatory and anticancer properties [76, 77] but might also cause inflammation [78]. In addition, from a broad perspective, this study found that certain active components might exert a wide range of pharmacological effects by targeting multiple targets, as shown in Figure 2 and Figure 3, which provides a theoretical basis for the streamlining of TCM prescriptions. The heat map clearly shows the likely mutual interaction between key components and hub targets determined by molecular docking, which provides a clue for the optimization of prescription compositions in the development of multitarget TCM medicines.

The focus of this research was to explore the mechanism of XSLJP in the treatment of gastritis, but as observed in many studies, inflammatory conditions can promote cancerous development, which in turn induces an inflammatory microenvironment that is more conducive to cancer progression [79]. Normal gastric cells often undergo inflammation after being invaded by infectious *Helicobacter pylori* and further develop chronic inflammation, which might deteriorate into gastric cancer if no treatments are applied in time and properly. The correlation between gastritis and gastric cancer is obvious because gastritis meets the characteristics of cancer-related inflammation regarding specific inflammatory mediators, including cytokines and chemokines [79]. The above-described analysis on predicting targets of the active components of XSLJP and their related pathways confirms the importance of cytokines and chemokines in gastritis drug therapy. Therefore, our study also indicates that XSLJP might have the potential to be further studied for the treatment of gastric cancer.

Conclusions

In this study, we identified 12 key active components and eight hub therapeutic targets of XSLJP in the treatment of gastritis through network pharmacology. Based on our comprehensive analysis of these active components and targets, we propose that the mechanism of XSLJP in the treatment of gastritis involves multiple targets and multiple pathways, which mainly include the TNF, JAK/STAT, MAPK, p53 and NO/VEGF signaling pathways. The potential mutual interaction between core active ingredients, such as glepidotin A, glycitein, licochalcone α and formononetin, and hub targets, such as PTGS2, JUN, FOS and HIF1A, are worth further experimental research. This study provides new ideas for further exploring the detailed mechanism of XSLJP in the treatment of gastritis as well as a certain theoretical basis for further in-depth study of these ingredients, the optimization of compound prescriptions, the adjustment of clinical application schemes and even the development of new drugs.

Authorship contributions

ZH, JW, ZL and YL conceived and designed the experiments; ZL, TT, RY and XC collected the data; RY and XC performed the target prediction and the verification of the active components; TT performed the molecular docking simulations; ZL and TT constructed the network; JW, RY and XC prepared the figures; JW, ZL, TT, RY and XC analyzed the data and prepared the tables; JW and TT performed the pathway analyses; JW, ZL and TT wrote the manuscript; YL and ZH guided the writing of the manuscript; and ZH revised the manuscript and provided financial support. Additionally, all the authors read and approved the final manuscript.

Conflict of interest

The authors declare no conflict of interest.

Data Availability

The data that support the findings of this study are openly available in the TCMSP database (http://tcmspw.com/tcmsp.php), the SwissTargetPrediction (STP) database (http://www.swisstargetprediction.ch/), the STITCH database (http://stitch.embl.de/) and the DisGeNET database (https://www.disgenet.org/).

Funding sources

This work was supported by the Key Discipline Construction Project of Guangdong Medical University [4SG22004G] and the Higher Education Reform Project of Guangdong Province [2019268].

Acknowledgements

We thank American Journal Experts for their help in revising the English grammar.

Supplementary Materials:

Table 1S: Information on 118 active components in Xiangsha Liujun Pill.

Table 2S: Information on 180 gastritis-related targets.

Table 3S: Information on 327 predictive targets based on 118 active components.

Table 4S: Information on 21 experimentally verified targets obtained by searching the PubMed database.

Table 5S: LibDock results of the 118 active components and five targets that have not been verified experimentally (as determined by a search of the PubMed database).

Figure 1S: Detailed information on the TNF signaling pathway.

Figure 2S: Detailed information on the JAK-STAT signaling pathway.

Figure 3S: Detailed information on the MAPK signaling pathway.

Figure 4S: Detailed information on the p53 signaling pathway.

Figure 5S: Detailed information on the NO/VEGF signaling pathway.

References:

[1] S. Chen, X. Tian, “Liujunzi decoction for diabetic mild gastroparesis:a Meta analysis.,” *Chinese Journal of clinical research*, vol. 27, no. 08, pp. 913-918, 2014.

[2] Z. Pan, X. Pan, X. Pan, “The Clinical application of Xiangshaliujunzi Decoction in stomach illness.,” *Journal of Traditional Chinese Medicine*, vol. 50, pp. 65, 2009.

[3] B. Cai, D. Wei, “Clinical observation of Xiangsha Liujun pill in treating 77 cases of chronic gastritis,” *Fujian Journal of Traditional Chinese Medicine*, vol. 37, no. 05, pp. 11-12, 2006.

[4] B. Yu, “Xiangsha Liujunzi Pill Combined with omeprazole in Treating 65 cases of chronic atrophic gastritis,” *Journal of Sichuan of Traditional Chinese Medicine*, vol. 32, no. 02, pp. 95-96, 2014.

[5] F. Zhang, C. Kang, X. Hu, S. Li, P. Li, “Observation on Efficacy of Xiangsha Liujun Pills Combined with Pantoprazole in Treatment of Chronic Atrophic Gastritis,” *Evaluation and Analysis of Drug-Use in Hospitals of China*, vol. 19, no. 07, pp. 832-833+837, 2019.

[6] Z.-Q. Lin, D.-X. Wang, S.-S. Hong, X.-Y. Fu, “Effects of Xiangsha Liujunzi decoction on TLR signal pathway in gastric mucosa tissues of rats with Helicobacter pylori-induced chronic atrophic gastritis,” *China journal of Chinese materia medica*, vol. 41, no. 16, pp. 3078-3083, 2016.

[7] J. Huang, Y. Mao, Q. Pei, Y. Liu, W. Zhou, “Influence of Xiangsha Liujun Pill to Clinical Efficacy and Gastrointestinal Hormones in the Treatment of

Chronic Renal Failure of Qi Deficiency of Spleen and Kidney," *Acta Chinese Medicine and Pharmacology*, vol. 47, no. 06, pp. 83-86, 2019.
[8] I. S. Ok, S. H. Kim, B. K. Kim, J. C. Lee, Y. C. Lee, "Pinellia ternata, Citrus reticulata, and their combinational prescription inhibit eosinophil infiltration and airway hyperresponsiveness by suppressing CCR3+ and Th2 cytokines production in the ovalbumin-induced asthma model," *Mediators Inflamm*, vol. 2009, pp. 413270, 2009.
[9] X. Liu, X. Wang, X. Xu, X. Zhang, "Purification, antitumor and anti-inflammation activities of an alkali-soluble and carboxymethyl polysaccharide CMP33 from Poria cocos," *Int J Biol Macromol*, vol. 127, no. 2019, pp. 39-47, 2019.
[10] G. Ji, R. Chen, J. Zheng, "Atractylenolide I inhibits lipopolysaccharide-induced inflammatory responses via mitogen-activated protein kinase pathways in RAW264.7 cells," *Immunopharmacol Immunotoxicol*, vol. 36, no. 6, pp. 420-425, 2014.
[11] H. Yuan, Q. Ma, H. Cui, et al., "How Can Synergism of Traditional Medicines Benefit from Network Pharmacology?," *Molecules*, vol. 22, no. 7, 2017.
[12] W. Y. Lee, C. Y. Lee, Y. S. Kim, C. E. Kim, "The Methodological Trends of Traditional Herbal Medicine Employing Network Pharmacology," *Biomolecules*, vol. 9, no. 8, pp. 362, 2019.
[13] J. Huang, F. Cheung, H. Y. Tan, et al., "Identification of the active compounds and significant pathways of yinchenhao decoction based on network pharmacology," *Mol Med Rep*, vol. 16, no. 4, pp. 4583-4592, 2017.
[14] J. Ru, P. Li, J. Wang, et al., "TCMSP: a database of systems pharmacology for drug discovery from herbal medicines," *J Cheminform*, vol. 6, pp. 13, 2014.
[15] A. Daina, O. Michielin, V. Zoete, "SwissTargetPrediction: updated data and new features for efficient prediction of protein targets of small molecules," *Nucleic Acids Res*, vol. 47, no. W1, pp. W357-w364, 2019.
[16] D. Szklarczyk, A. Santos, C. von Mering, et al., "STITCH 5: augmenting protein-chemical interaction networks with tissue and affinity data," *Nucleic Acids Res*, vol. 44, no. D1, pp. D380-384, 2016.
[17] J. Piñero, J. M. Ramírez-Anguita, J. Saüch-Pitarch, et al., "The DisGeNET knowledge platform for disease genomics: 2019 update," *Nucleic Acids Res*, vol. 48, no. D1, pp. D845-d855, 2020.
[18] D. S. BIOVIA, "Discovery Studio Modeling Environment, Release 2020," *San Diego: Dassault Systèmes*, 2019.
[19] D. Szklarczyk, A. L. Gable, D. Lyon, et al., "STRING v11: protein-protein association networks with increased coverage, supporting

functional discovery in genome-wide experimental datasets," *Nucleic Acids Res*, vol. 47, no. D1, pp. D607-d613, 2019.
[20] P. Shannon, A. Markiel, O. Ozier, et al., "Cytoscape: a software environment for integrated models of biomolecular interaction networks," *Genome Res*, vol. 13, no. 11, pp. 2498-2504, 2003.
[21] W. Huang da, B. T. Sherman, R. A. Lempicki, "Systematic and integrative analysis of large gene lists using DAVID bioinformatics resources," *Nat Protoc*, vol. 4, no. 1, pp. 44-57, 2009.
[22] S. Kim, J. Chen, T. Cheng, et al., "PubChem in 2021: new data content and improved web interfaces," *Nucleic Acids Res*, vol. 49, no. D1, pp. D1388-d1395, 2021.
[23] U. Consortium, "UniProt: the universal protein knowledgebase in 2021," *Nucleic Acids Res*, vol. 49, no. D1, pp. D480-D489, 2021.
[24] S. K. Burley, C. Bhikadiya, C. Bi, et al., "RCSB Protein Data Bank: powerful new tools for exploring 3D structures of biological macromolecules for basic and applied research and education in fundamental biology, biomedicine, biotechnology, bioengineering and energy sciences," *Nucleic Acids Res*, vol. 49, no. D1, pp. D437-d451, 2021.
[25] S. N. Rao, M. S. Head, A. Kulkarni, J. M. LaLonde, "Validation studies of the site-directed docking program LibDock," *J Chem Inf Model*, vol. 47, no. 6, pp. 2159-2171, 2007.
[26] J. Koska, V. Z. Spassov, A. J. Maynard, et al., "Fully automated molecular mechanics based induced fit protein-ligand docking method," *J Chem Inf Model*, vol. 48, no. 10, pp. 1965-1973, 2008.
[27] Z. Xu, X. Fan, S. Wang, "Chemical Components and Advances in Research Progress of Extracting Volatile Oil from Aucklandiae Lappa Decne," *Guangdong Chemical Industry*, vol. 44, no. 03, pp. 77-78, 2017.
[28] L. Li, W. Tian, Y. Liu, et al., "Research Progress on Chemical Constituents and Pharmacological Effects of Amomum villosum," *Progress in Modern Biomedicine*, vol. 18, no. 22, pp. 4390-4396, 2018.
[29] S. Gu, W. Kong, T. Zhang, et al., "Advances on Chemical Compositions, Pharmacological Effects and Compound Clinical Applications of Atractylodes macrocephala Koidz.," *Chinese Archives of Traditional Chinese Medicine*, vol. 38, no. 01, pp. 69-73, 2020.
[30] M. Rugge, G. Pennelli, E. Pilozzi, et al., "Gastritis: the histology report," *Dig Liver Dis*, vol. 43, pp. S373-384, 2011.
[31] A. Tatsuguchi, S. Hoshino, N. Kawami, et al., "Influence of hypergastrinemia secondary to long-term proton pump inhibitor treatment on ECL cell tumorigenesis in human gastric mucosa," *Pathol Res Pract*, vol. 216, no. 10, pp. 153113, 2020.

[32] E. J. Gong, D. H. Kim, J. Y. Ahn, et al., “Effects of Proton Pump Inhibitor on the Distribution of Helicobacter pylori and Associated Gastritis in Patients with Gastric Atrophy,” *Digestion*, vol. 101, no. 3, pp. 279-286, 2020.
[33] T. Kobayashi, T. Yabana, “Mechanisms of direct gastric mucosal damage by NSAIDs,” *Nihon Rinsho*, vol. 65, no. 10, pp. 1803-1806, 2007.
[34] P. Correa, “Gastric cancer: overview,” *Gastroenterol Clin North Am*, vol. 42, no. 2, pp. 211-217, 2013.
[35] W. Zhang, Y. Huai, Z. Miao, A. Qian, Y. Wang, “Systems Pharmacology for Investigation of the Mechanisms of Action of Traditional Chinese Medicine in Drug Discovery,” *Front Pharmacol*, vol. 10, pp. 743, 2019.
[36] Y. Lin, D. Tan, Q. Kan, Z. Xiao, Z. Jiang, “The Protective Effect of Naringenin on Airway Remodeling after Mycoplasma Pneumoniae Infection by Inhibiting Autophagy-Mediated Lung Inflammation and Fibrosis,” *Mediators Inflamm*, vol. 2018, pp. 8753894, 2018.
[37] K. Taniguchi, M. Karin, “NF-κB, inflammation, immunity and cancer: coming of age,” *Nat Rev Immunol*, vol. 18, no. 5, pp. 309-324, 2018.
[38] Y. Mao, Q. Zhao, S. Yin, X. Ding, H. Wang, “Genome-wide expression profiling and bioinformatics analysis of deregulated genes in human gastric cancer tissue after gastroscopy,” *Asia Pac J Clin Oncol*, vol. 14, no. 2, pp. e29-e36, 2018.
[39] N. Xu, J. An, “Formononetin ameliorates mast cell-mediated allergic inflammation via inhibition of histamine release and production of pro-inflammatory cytokines,” *Exp Ther Med*, vol. 14, no. 6, pp. 6201-6206, 2017.
[40] Y. Wu, F. Chen, X. Huang, et al., “Berberine (BBR) Attenuated Palmitic Acid (PA)-Induced Lipotoxicity in Human HK-2 Cells by Promoting Peroxisome Proliferator-Activated Receptor α (PPAR-α),” *Med Sci Monit*, vol. 25, pp. 7702-7708, 2019.
[41] J. E. Darnell, Jr., “STATs and gene regulation,” *Science*, vol. 277, no. 5332, pp. 1630-1635, 1997.
[42] H. Yu, D. Pardoll, R. Jove, “STATs in cancer inflammation and immunity: a leading role for STAT3,” *Nat Rev Cancer*, vol. 9, no. 11, pp. 798-809, 2009.
[43] T. Mori, T. Miyamoto, H. Yoshida, et al., “IL-1β and TNFα-initiated IL-6-STAT3 pathway is critical in mediating inflammatory cytokines and RANKL expression in inflammatory arthritis,” *Int Immunol*, vol. 23, no. 11, pp. 701-712, 2011.
[44] R. Catlett-Falcone, T. H. Landowski, M. M. Oshiro, et al.,

“Constitutive activation of Stat3 signaling confers resistance to apoptosis in human U266 myeloma cells,” *Immunity*, vol. 10, no. 1, pp. 105-115, 1999.
[45] S. Smola, C. Trimble, P. L. Stern, “Human papillomavirus-driven immune deviation: challenge and novel opportunity for immunotherapy,” *Ther Adv Vaccines*, vol. 5, no. 3, pp. 69-82, 2017.
[46] D. M. Mosser, X. Zhang, “Interleukin-10: new perspectives on an old cytokine,” *Immunol Rev*, vol. 226, pp. 205-218, 2008.
[47] K. W. Moore, R. de Waal Malefyt, R. L. Coffman, A. O'Garra, “Interleukin-10 and the interleukin-10 receptor,” *Annu Rev Immunol*, vol. 19, pp. 683-765, 2001.
[48] W. Tan, M. Pan, H. Liu, et al., “Ergosterol peroxide inhibits ovarian cancer cell growth through multiple pathways,” *Onco Targets Ther*, vol. 10, pp. 3467-3474, 2017.
[49] N. Sp, D. Y. Kang, D. H. Kim, et al., “Nobiletin Inhibits CD36-Dependent Tumor Angiogenesis, Migration, Invasion, and Sphere Formation Through the Cd36/Stat3/Nf-Kb Signaling Axis,” *Nutrients*, vol. 10, no. 6, pp. 772, 2018.
[50] N. Sp, D. Y. Kang, Y. H. Joung, et al., “Nobiletin Inhibits Angiogenesis by Regulating Src/FAK/STAT3-Mediated Signaling through PXN in ER$^+$ Breast Cancer Cells,” *Int J Mol Sci*, vol. 18, no. 5, pp. 935, 2017.
[51] S. Namkoong, J. Sung, J. Yang, et al., “Nobiletin Attenuates the Inflammatory Response Through Heme Oxygenase-1 Induction in the Crosstalk Between Adipocytes and Macrophages,” *J Med Food*, vol. 20, no. 9, pp. 873-881, 2017.
[52] V. M. Devraj, S. K. Vemuri, R. R. Banala, et al., “Evaluation of Anti-inflammatory and Regenerative Efficiency of Naringin and Naringenin in Degenerated Human Nucleus Pulposus Cells: Biological and Molecular Modeling Studies,” *Asian Spine J*, vol. 13, no. 6, pp. 875-889, 2019.
[53] B. Canovas, A. R. Nebreda, “Diversity and versatility of p38 kinase signalling in health and disease,” *Nat Rev Mol Cell Biol*, pp. 1-21, 2021.
[54] A. Cuadrado, A. R. Nebreda, “Mechanisms and functions of p38 MAPK signalling,” *Biochem J*, vol. 429, no. 3, pp. 403-417, 2010.
[55] E. F. Wagner, A. R. Nebreda, “Signal integration by JNK and p38 MAPK pathways in cancer development,” *Nat Rev Cancer*, vol. 9, no. 8, pp. 537-549, 2009.
[56] T. Korn, E. Bettelli, M. Oukka, V. K. Kuchroo, “IL-17 and Th17 Cells,” *Annu Rev Immunol*, vol. 27, pp. 485-517, 2009.
[57] E. D. S. Santos, K. A. B. Nogueira, L. C. C. Fernandes, et al., “EGFR targeting for cancer therapy: Pharmacology and immunoconjugates with drugs and nanoparticles,” *Int J Pharm*, vol. 592, pp. 120082, 2021.

[58] X. Liu, P. Wang, C. Zhang, Z. Ma, “Epidermal growth factor receptor (EGFR): A rising star in the era of precision medicine of lung cancer,” *Oncotarget*, vol. 8, no. 30, pp. 50209-50220, 2017.
[59] Q. Liu, X. Xu, M. Zhao, et al., “Berberine induces senescence of human glioblastoma cells by downregulating the EGFR-MEK-ERK signaling pathway,” *Mol Cancer Ther*, vol. 14, no. 2, pp. 355-363, 2015.
[60] X. Yu, F. Gao, W. Li, et al., “Formononetin inhibits tumor growth by suppression of EGFR-Akt-Mcl-1 axis in non-small cell lung cancer,” *J Exp Clin Cancer Res*, vol. 39, no. 1, pp. 62, 2020.
[61] N. Barabutis, A. V. Schally, A. Siejka, “P53, GHRH, inflammation and cancer,” *EBioMedicine*, vol. 37, pp. 557-562, 2018.
[62] E. M. Kim, C. H. Jung, J. Kim, et al., “The p53/p21 Complex Regulates Cancer Cell Invasion and Apoptosis by Targeting Bcl-2 Family Proteins,” *Cancer Res*, vol. 77, no. 11, pp. 3092-3100, 2017.
[63] Y. Xiong, G. J. Hannon, H. Zhang, et al., “p21 is a universal inhibitor of cyclin kinases,” *Nature*, vol. 366, no. 6456, pp. 701-704, 1993.
[64] M. L. Smith, J. M. Ford, M. C. Hollander, et al., “p53-mediated DNA repair responses to UV radiation: studies of mouse cells lacking p53, p21, and/or gadd45 genes,” *Mol Cell Biol*, vol. 20, no. 10, pp. 3705-3714, 2000.
[65] S. Tulsyan, R. D. Mittal, B. Mittal, “The effect of ABCB1 polymorphisms on the outcome of breast cancer treatment,” *Pharmgenomics Pers Med*, vol. 9, pp. 47-58, 2016.
[66] M. G. Sabbieti, D. Agas, G. Santoni, et al., “Involvement of p53 in phthalate effects on mouse and rat osteoblasts,” *J Cell Biochem*, vol. 107, no. 2, pp. 316-327, 2009.
[67] Y. Ye, H. Wang, J. H. Chu, et al., “Atractylenolide II induces G1 cell-cycle arrest and apoptosis in B16 melanoma cells,” *J Ethnopharmacol*, vol. 136, no. 1, pp. 279-282, 2011.
[68] L. Fu, W. Chen, W. Guo, et al., “Berberine Targets AP-2/hTERT, NF-κB/COX-2, HIF-1α/VEGF and Cytochrome-c/Caspase Signaling to Suppress Human Cancer Cell Growth,” *PLoS One*, vol. 8, no. 7, pp. e69240, 2013.
[69] K. Takeuchi, K. Amagase, “Roles of Cyclooxygenase, Prostaglandin E2 and EP Receptors in Mucosal Protection and Ulcer Healing in the Gastrointestinal Tract,” *Curr Pharm Des*, vol. 24, no. 18, pp. 2002-2011, 2018.
[70] K. Echizen, H. Oshima, M. Nakayama, M. Oshima, “The inflammatory microenvironment that promotes gastrointestinal cancer development and invasion,” *Adv Biol Regul*, vol. 68, pp. 39-45, 2018.

[71] S. K. L. Ong, M. K. Shanmugam, L. Fan, et al., “Focus on Formononetin: Anticancer Potential and Molecular Targets,” *Cancers (Basel)*, vol. 11, no. 5, pp. 611, 2019.
[72] A. Ahluwalia, A. S. Tarnawski, “Critical role of hypoxia sensor--HIF-1α in VEGF gene activation. Implications for angiogenesis and tissue injury healing,” *Curr Med Chem*, vol. 19, no. 1, pp. 90-97, 2012.
[73] J. Shin, H. J. Lee, D. B. Jung, et al., “Suppression of STAT3 and HIF-1 alpha mediates anti-angiogenic activity of betulinic acid in hypoxic PC-3 prostate cancer cells,” *PLoS One*, vol. 6, no. 6, pp. e21492, 2011.
[74] J. Chen, A. Creed, A. Y. Chen, et al., “Nobiletin suppresses cell viability through AKT pathways in PC-3 and DU-145 prostate cancer cells,” *BMC Pharmacol Toxicol*, vol. 15, pp. 59, 2014.
[75] A. Okuda-Tanino, D. Sugawara, T. Tashiro, et al., “Licochalcones extracted from Glycyrrhiza inflata inhibit platelet aggregation accompanied by inhibition of COX-1 activity,” *PLoS One*, vol. 12, no. 3, pp. e0173628, 2017.
[76] W. C. Huang, T. H. Tsai, L. T. Chuang, et al., “Anti-bacterial and anti-inflammatory properties of capric acid against Propionibacterium acnes: a comparative study with lauric acid,” *J Dermatol Sci*, vol. 73, no. 3, pp. 232-240, 2014.
[77] D. L. Sheela, A. Narayanankutty, P. A. Nazeem, A. C. Raghavamenon, S. R. Muthangaparambil, “Lauric acid induce cell death in colon cancer cells mediated by the epidermal growth factor receptor downregulation: An in silico and in vitro study,” *Hum Exp Toxicol*, vol. 38, no. 7, pp. 753-761, 2019.
[78] D. M. Rocha, A. P. Caldas, L. L. Oliveira, J. Bressan, H. H. Hermsdorff, “Saturated fatty acids trigger TLR4-mediated inflammatory response,” *Atherosclerosis*, vol. 244, pp. 211-215, 2016.
[79] A. Mantovani, P. Allavena, A. Sica, F. Balkwill, “Cancer-related inflammation,” *Nature*, vol. 454, no. 7203, pp. 436-444, 2008.
[80] Z. Zhang, B. Li, J. Huang, et al., “A Network Pharmacology Analysis of the Active Components of the Traditional Chinese Medicine Zuojinwan in Patients with Gastric Cancer,” *Med Sci Monit*, vol. 26, pp. e923327, 2020.
[81] G. Moroy, E. Bourguet, M. Decarme, et al., “Inhibition of human leukocyte elastase, plasmin and matrix metalloproteinases by oleic acid and oleoyl-galardin derivative(s),” *Biochem Pharmacol*, vol. 81, no. 5, pp. 626-635, 2011.
[82] W. Li, W. Zhi, F. Liu, et al., “Atractylenolide I restores HO-1 expression and inhibits Ox-LDL-induced VSMCs proliferation, migration and inflammatory responses in vitro,” *Exp Cell Res*, vol. 353, no. 1, pp. 26-34,

2017.
[83] H. J. Kwak, D. Yang, Y. Hwang, H. S. Jun, H. G. Cheon, “Baicalein protects rat insulinoma INS-1 cells from palmitate-induced lipotoxicity by inducing HO-1,” *PLoS One*, vol. 12, no. 4, pp. e0176432, 2017.
[84] J. H. Campbell, J. J. Heikkila, “Effect of hemin, baicalein and heme oxygenase-1 (HO-1) enzyme activity inhibitors on Cd-induced accumulation of HO-1, HSPs and aggresome-like structures in Xenopus kidney epithelial cells,” *Comp Biochem Physiol C Toxicol Pharmacol*, vol. 210, pp. 1-17, 2018.
[85] D. Li, G. Shi, J. Wang, et al., “Baicalein ameliorates pristane-induced lupus nephritis via activating Nrf2/HO-1 in myeloid-derived suppressor cells,” *Arthritis Res Ther*, vol. 21, no. 1, pp. 105, 2019.
[86] Z. Zhang, W. Cui, G. Li, et al., “Baicalein protects against 6-OHDA-induced neurotoxicity through activation of Keap1/Nrf2/HO-1 and involving PKCα and PI3K/AKT signaling pathways,” *J Agric Food Chem*, vol. 60, no. 33, pp. 8171-8182, 2012.
[87] Y. C. Chen, J. M. Chow, C. W. Lin, C. Y. Wu, S. C. Shen, “Baicalein inhibition of oxidative-stress-induced apoptosis via modulation of ERKs activation and induction of HO-1 gene expression in rat glioma cells C6,” *Toxicol Appl Pharmacol*, vol. 216, no. 2, pp. 263-273, 2006.
[88] E. O. Choi, J. W. Jeong, C. Park, et al., “Baicalein protects C6 glial cells against hydrogen peroxide-induced oxidative stress and apoptosis through regulation of the Nrf2 signaling pathway,” *Int J Mol Med*, vol. 37, no. 3, pp. 798-806, 2016.
[89] A. Liu, L. Huang, E. Guo, et al., “Baicalein pretreatment reduces liver ischemia/reperfusion injury via induction of autophagy in rats,” *Sci Rep*, vol. 6, pp. 25042, 2016.
[90] Y. H. Choi, “Activation of the Nrf2/HO-1 signaling pathway contributes to the protective effects of coptisine against oxidative stress-induced DNA damage and apoptosis in HaCaT keratinocytes,” *Gen Physiol Biophys*, vol. 38, no. 4, pp. 281-294, 2019.
[91] D. Lee, J. Bae, Y. K. Kim, et al., “Inhibitory effects of berberine on lipopolysaccharide-induced inducible nitric oxide synthase and the high-mobility group box 1 release in macrophages,” *Biochem Biophys Res Commun*, vol. 431, no. 3, pp. 506-511, 2013.
[92] L. Mao, Q. Chen, K. Gong, et al., “Berberine decelerates glucose metabolism via suppression of mTOR-dependent HIF-1α protein synthesis in colon cancer cells,” *Oncol Rep*, vol. 39, no. 5, pp. 2436-2442, 2018.
[93] J. Feng, J. Luo, L. Deng, et al., “Naringenin-induced HO-1 ameliorates high glucose or free fatty acids-associated apoptosis via PI3K and JNK/Nrf2 pathways in human umbilical vein endothelial cells,” *Int*

Immunopharmacol, vol. 75, pp. 105769, 2019.
[94] Y. Jin, H. Wang, “Naringenin Inhibit the Hydrogen Peroxide-Induced SH-SY5Y Cells Injury Through Nrf2/HO-1 Pathway,” *Neurotox Res*, vol. 36, no. 4, pp. 796-805, 2019.
[95] H. Lin, S. Shen, Y. Chen, “Anti-inflammatory effect of heme oxygenase 1: glycosylation and nitric oxide inhibition in macrophages,” *J Cell Physiol*, vol. 202, no. 2, pp. 579-590, 2005.
[96] M. R. de Oliveira, C. M. B. Andrade, C. R. Fürstenau, “Naringenin Exerts Anti-inflammatory Effects in Paraquat-Treated SH-SY5Y Cells Through a Mechanism Associated with the Nrf2/HO-1 Axis,” *Neurochem Res*, vol. 43, no. 4, pp. 894-903, 2018.
[97] S. Chen, Y. Ding, W. Tao, et al., “Naringenin inhibits TNF-α induced VSMC proliferation and migration via induction of HO-1,” *Food Chem Toxicol*, vol. 50, no. 9, pp. 3025-3031, 2012.
[98] H. Y. Lin, S. H. Juan, S. C. Shen, F. L. Hsu, Y. C. Chen, “Inhibition of lipopolysaccharide-induced nitric oxide production by flavonoids in RAW264.7 macrophages involves heme oxygenase-1,” *Biochem Pharmacol*, vol. 66, no. 9, pp. 1821-1832, 2003.
[99] Z. Qi, Y. Xu, Z. Liang, et al., “Naringin ameliorates cognitive deficits via oxidative stress, proinflammatory factors and the PPARγ signaling pathway in a type 2 diabetic rat model,” *Mol Med Rep*, vol. 12, no. 5, pp. 7093-7101, 2015.
[100] Y. H. Lee, N. H. Lee, G. Bhattarai, et al., “Anti-inflammatory effect of pachymic acid promotes odontoblastic differentiation via HO-1 in dental pulp cells,” *Oral Dis*, vol. 19, no. 2, pp. 193-199, 2013.
[101] X. Xuan, Z. Sun, C. Yu, et al., “Network pharmacology-based study of the protective mechanism of conciliatory anti-allergic decoction on asthma,” *Allergol Immunopathol (Madr)*, vol. 48, no. 5, pp. 441-449, 2020.
[102] L. Fang, M. Liu, L. Cai, “Hederagenin inhibits proliferation and promotes apoptosis of cervical cancer CaSki cells by blocking STAT3 pathway,” *Chinese journal of cellular and molecular immunology*, vol. 35, no. 2, pp. 140-145, 2019.
[103] M. H. Cha, I. C. Kim, B. H. Lee, Y. Yoon, “Baicalein inhibits adipocyte differentiation by enhancing COX-2 expression,” *J Med Food*, vol. 9, no. 2, pp. 145-153, 2006.
[104] J. Huai, X. Zhao, S. Wang, et al., “Characterization and screening of cyclooxygenase-2 inhibitors from Zi-shen pill by affinity ultrafiltration-ultra performance liquid chromatography mass spectrometry,” *J Ethnopharmacol*, vol. 241, pp. 111900, 2019.
[105] H. M. Hussien, A. Abd-Elmegied, D. A. Ghareeb, et al.,

“Neuroprotective effect of berberine against environmental heavy metals-induced neurotoxicity and Alzheimer's-like disease in rats,” *Food Chem Toxicol*, vol. 111, pp. 432-444, 2018.
[106] Y. Liu, Y. Liu, W. Zhang, et al., “Network Pharmacology-Based Strategy to Investigate the Pharmacological Mechanisms of Ginkgo biloba Extract for Aging,” *Evid Based Complement Alternat Med*, vol. 2020, pp. 8508491, 2020.
[107] M. M. Ranjbar, V. Assadolahi, M. Yazdani, D. Nikaein, B. Rashidieh, “Virtual Dual inhibition of COX-2 / 5-LOX enzymes based on binding properties of alpha-amyrins, the anti-inflammatory compound as a promising anti-cancer drug,” *Excli j*, vol. 15, pp. 238-245, 2016.
[108] X. Ruan, P. Du, K. Zhao, et al., “Mechanism of Dayuanyin in the treatment of coronavirus disease 2019 based on network pharmacology and molecular docking,” *Chin Med*, vol. 15, pp. 62, 2020.
[109] J. Peng, Y. C. Lv, P. P. He, et al., “Betulinic acid downregulates expression of oxidative stress-induced lipoprotein lipase via the PKC/ERK/c-Fos pathway in RAW264.7 macrophages,” *Biochimie*, vol. 119, pp. 192-203, 2015.
[110] W. Wang, M. Li, M. Luo, et al., “Naringenin inhibits osteoclastogenesis through modulation of helper T cells-secreted IL-4,” *J Cell Biochem*, vol. 119, no. 2, pp. 2084-2093, 2018.
[111] S. Huang, Z. Zhang, W. Li, et al., “Network Pharmacology-Based Prediction and Verification of the Active Ingredients and Potential Targets of Zuojinwan for Treating Colorectal Cancer,” *Drug Des Devel Ther*, vol. 14, pp. 2725-2740, 2020.
[112] Y. Huang, Z. Miao, Y. Hu, et al., “Baicalein reduces angiogenesis in the inflammatory microenvironment via inhibiting the expression of AP-1,” *Oncotarget*, vol. 8, no. 1, pp. 883-899, 2017.
[113] W. Liu, Y. Fan, C. Tian, et al., “Deciphering the Molecular Targets and Mechanisms of HGWD in the Treatment of Rheumatoid Arthritis via Network Pharmacology and Molecular Docking,” *Evid Based Complement Alternat Med*, vol. 2020, pp. 7151634, 2020.
[114] H. Li, C. He, J. Wang, et al., “Berberine activates peroxisome proliferator-activated receptor gamma to increase atherosclerotic plaque stability in Apoe(-/-) mice with hyperhomocysteinemia,” *J Diabetes Investig*, vol. 7, no. 6, pp. 824-832, 2016.
[115] C. Guan, S. Qiao, Q. Lv, et al., “Orally administered berberine ameliorates bleomycin-induced pulmonary fibrosis in mice through promoting activation of PPAR-γ and subsequent expression of HGF in colons,” *Toxicol Appl Pharmacol*, vol. 343, pp. 1-15, 2018.

[116] J. Tu, X. X. Luo, B. T. Li, Y. Li, G. L. Xu, “Effects of berberine on mRNA expression levels of PPARγ and adipocytokines in insulin-resistant adipocytes,” *China journal of Chinese materia medica*, vol. 41, no. 11, pp. 1983-1989, 2016.
[117] Y. Y. Wu, X. M. Huang, J. Liu, et al., “Functional study of the upregulation of miRNA-27a and miRNA-27b in 3T3-L1 cells in response to berberine,” *Mol Med Rep*, vol. 14, no. 3, pp. 2725-2731, 2016.
[118] F. L. Chen, Z. H. Yang, Y. Liu, et al., “Berberine inhibits the expression of TNFalpha, MCP-1, and IL-6 in AcLDL-stimulated macrophages through PPARgamma pathway,” *Endocrine*, vol. 33, no. 3, pp. 331-337, 2008.
[119] A. W. Feng, W. Gao, G. R. Zhou, et al., “Berberine ameliorates COX-2 expression in rat small intestinal mucosa partially through PPARγ pathway during acute endotoxemia,” *Int Immunopharmacol*, vol. 12, no. 1, pp. 182-188, 2012.
[120] Y. Chen, Y. Li, Y. Wang, Y. Wen, C. Sun, “Berberine improves free-fatty-acid-induced insulin resistance in L6 myotubes through inhibiting peroxisome proliferator-activated receptor gamma and fatty acid transferase expressions,” *Metabolism*, vol. 58, no. 12, pp. 1694-1702, 2009.
[121] V. S. Grytting, B. P. Olderbø, J. A. Holme, et al., “Di-n-butyl phthalate modifies PMA-induced macrophage differentiation of THP-1 monocytes via PPARγ,” *Toxicol In Vitro*, vol. 54, pp. 168-177, 2019.
[122] T. Nie, S. Zhao, L. Mao, et al., “The natural compound, formononetin, extracted from Astragalus membranaceus increases adipocyte thermogenesis by modulating PPARγ activity,” *Br J Pharmacol*, vol. 175, no. 9, pp. 1439-1450, 2018.
[123] G. Brusotti, R. Montanari, D. Capelli, et al., “Betulinic acid is a PPARγ antagonist that improves glucose uptake, promotes osteogenesis and inhibits adipogenesis,” *Sci Rep*, vol. 7, no. 1, pp. 5777, 2017.
[124] W. Jingbo, C. Aimin, W. Qi, L. Xin, L. Huaining, “Betulinic acid inhibits IL-1β-induced inflammation by activating PPAR-γ in human osteoarthritis chondrocytes,” *Int Immunopharmacol*, vol. 29, no. 2, pp. 687-692, 2015.
[125] A. K. Singh, V. Raj, A. K. Keshari, et al., “Isolated mangiferin and naringenin exert antidiabetic effect via PPAR(γ)/GLUT4 dual agonistic action with strong metabolic regulation,” *Chem Biol Interact*, vol. 280, pp. 33-44, 2018.
[126] A. Nishina, D. Sato, J. Yamamoto, et al., “Antidiabetic-Like Effects of Naringenin-7-O-glucoside from Edible Chrysanthemum 'Kotobuki' and Naringenin by Activation of the PI3K/Akt Pathway and PPARγ,” *Chem*

Biodivers, vol. 16, no. 1, pp. e1800434, 2019.
[127] J. Zhang, H. Qiu, J. Huang, et al., "EETs/PPARs activation together mediates the preventive effect of naringenin in high glucose-induced cardiomyocyte hypertrophy," *Biomed Pharmacother*, vol. 109, pp. 1498-1505, 2019.
[128] A. Giacoman-Martínez, F. J. Alarcón-Aguilar, A. Zamilpa, et al., "Triterpenoids from Hibiscus sabdariffa L. with PPARδ/γ Dual Agonist Action: In Vivo, In Vitro and In Silico Studies," *Planta Med*, vol. 85, no. 5, pp. 412-423, 2019.
[129] H. Qian, Q. Jin, Y. Liu, et al., "Study on the Multitarget Mechanism of Sanmiao Pill on Gouty Arthritis Based on Network Pharmacology," *Evid Based Complement Alternat Med*, vol. 2020, pp. 9873739, 2020.
[130] C. Zhu, T. Cai, Y. Jin, et al., "Artificial intelligence and network pharmacology based investigation of pharmacological mechanism and substance basis of Xiaokewan in treating diabetes," *Pharmacol Res*, vol. 159, pp. 104935, 2020.
[131] Y. Li, J. Ning, Y. Wang, et al., "Drug interaction study of flavonoids toward CYP3A4 and their quantitative structure activity relationship (QSAR) analysis for predicting potential effects," *Toxicol Lett*, vol. 294, pp. 27-36, 2018.
[132] Y. Zhao, B. H. Hellum, A. Liang, O. G. Nilsen, "Inhibitory Mechanisms of Human CYPs by Three Alkaloids Isolated from Traditional Chinese Herbs," *Phytother Res*, vol. 29, no. 6, pp. 825-834, 2015.
[133] P. Fasinu, Y. E. Choonara, R. A. Khan, et al., "Flavonoids and polymer derivatives as CYP3A4 inhibitors for improved oral drug bioavailability," *J Pharm Sci*, vol. 102, no. 2, pp. 541-555, 2013.
[134] S. K. Saha, A. R. Khuda-Bukhsh, "Berberine alters epigenetic modifications, disrupts microtubule network, and modulates HPV-18 E6-E7 oncoproteins by targeting p53 in cervical cancer cell HeLa: a mechanistic study including molecular docking," *Eur J Pharmacol*, vol. 744, pp. 132-146, 2014.
[135] S. Kumar, L. Jena, M. Sahoo, et al., "In Silico Docking to Explicate Interface between Plant-Originated Inhibitors and E6 Oncogenic Protein of Highly Threatening Human Papillomavirus 18," *Genomics Inform*, vol. 13, no. 2, pp. 60-67, 2015.
[136] B. Lu, M. Hu, K. Liu, J. Peng, "Cytotoxicity of berberine on human cervical carcinoma HeLa cells through mitochondria, death receptor and MAPK pathways, and in-silico drug-target prediction," *Toxicol In Vitro*, vol. 24, no. 6, pp. 1482-1490, 2010.

[137] S. K. Katiyar, S. M. Meeran, N. Katiyar, S. Akhtar, “p53 Cooperates berberine-induced growth inhibition and apoptosis of non-small cell human lung cancer cells in vitro and tumor xenograft growth in vivo,” *Mol Carcinog*, vol. 48, no. 1, pp. 24-37, 2009.
[138] F. Zheng, Q. Tang, J. Wu, et al., “p38α MAPK-mediated induction and interaction of FOXO3a and p53 contribute to the inhibited-growth and induced-apoptosis of human lung adenocarcinoma cells by berberine,” *J Exp Clin Cancer Res*, vol. 33, no. 1, pp. 36, 2014.
[139] Z. Liu, Q. Liu, B. Xu, et al., “Berberine induces p53-dependent cell cycle arrest and apoptosis of human osteosarcoma cells by inflicting DNA damage,” *Mutat Res*, vol. 662, no. 1-2, pp. 75-83, 2009.
[140] S. Kim, J. Han, N. Y. Kim, et al., “Effect of berberine on p53 expression by TPA in breast cancer cells,” *Oncol Rep*, vol. 27, no. 1, pp. 210-215, 2012.
[141] M. S. Choi, J. H. Oh, S. M. Kim, et al., “Berberine inhibits p53-dependent cell growth through induction of apoptosis of prostate cancer cells,” *Int J Oncol*, vol. 34, no. 5, pp. 1221-1230, 2009.
[142] M. S. Choi, D. Y. Yuk, J. H. Oh, et al., “Berberine inhibits human neuroblastoma cell growth through induction of p53-dependent apoptosis,” *Anticancer Res*, vol. 28, no. 6a, pp. 3777-3784, 2008.
[143] L. Y. Zhang, Y. L. Wu, X. H. Gao, F. Guo, “Mitochondrial protein cyclophilin-D-mediated programmed necrosis attributes to berberine-induced cytotoxicity in cultured prostate cancer cells,” *Biochem Biophys Res Commun*, vol. 450, no. 1, pp. 697-703, 2014.
[144] C. M. Saffarini, N. E. Heger, H. Yamasaki, et al., “Induction and persistence of abnormal testicular germ cells following gestational exposure to di-(n-butyl) phthalate in p53-null mice,” *J Androl*, vol. 33, no. 3, pp. 505-513, 2012.
[145] G. H. Jian, B. Z. Su, W. J. Zhou, H. Xiong, “Application of network pharmacology and molecular docking to elucidate the potential mechanism of Eucommia ulmoides-Radix Achyranthis Bidentatae against osteoarthritis,” *BioData Min*, vol. 13, pp. 12, 2020.
[146] A. Carazo Fernández, T. Smutny, L. Hyrsová, K. Berka, P. Pavek, “Chrysin, baicalein and galangin are indirect activators of the human constitutive androstane receptor (CAR),” *Toxicol Lett*, vol. 233, no. 2, pp. 68-77, 2015.
[147] M. Kim, K. H. Park, Y. B. Kim, “Identifying Active Compounds and Targets of Fritillariae thunbergii against Influenza-Associated Inflammation by Network Pharmacology Analysis and Molecular Docking,” *Molecules*, vol. 25, no. 17, 2020.

[148] Z. Bing, Z. Cheng, D. Shi, et al., “Investigate the mechanisms of Chinese medicine Fuzhengkangai towards EGFR mutation-positive lung adenocarcinomas by network pharmacology,” *BMC Complement Altern Med*, vol. 18, no. 1, pp. 293, 2018.
[149] K. E. Adewole, A. A. Ishola, “Phytosterols and triterpenes from Morinda lucida Benth (Rubiaceae) as potential inhibitors of anti-apoptotic BCL-XL, BCL-2, and MCL-1: an in-silico study,” *J Recept Signal Transduct Res*, vol. 39, no. 1, pp. 87-97, 2019.
[150] A. Triantafyllou, I. Mylonis, G. Simos, S. Bonanou, A. Tsakalof, “Flavonoids induce HIF-1alpha but impair its nuclear accumulation and activity,” *Free Radic Biol Med*, vol. 44, no. 4, pp. 657-670, 2008.
[151] X. Ma, M. Yu, C. Hao, W. Yang, “Identifying Synergistic Mechanisms of Multiple Ingredients in Shuangbai Tablets against Proteinuria by Virtual Screening and a Network Pharmacology Approach,” *Evid Based Complement Alternat Med*, vol. 2020, pp. 1027271, 2020.
[152] C. Wang, H. Duan, L. He, “Absorption kinetics of atractylenolide I in intestines of rats,” *China journal of Chinese materia medica*, vol. 34, no. 11, pp. 1430-1434, 2009.
[153] Y. Q. Shan, Y. P. Zhu, J. Pang, et al., “Tetrandrine potentiates the hypoglycemic efficacy of berberine by inhibiting P-glycoprotein function,” *Biol Pharm Bull*, vol. 36, no. 10, pp. 1562-1569, 2013.
[154] W. Ma, S. Feng, X. Yao, et al., “Nobiletin enhances the efficacy of chemotherapeutic agents in ABCB1 overexpression cancer cells,” *Sci Rep*, vol. 5, pp. 18789, 2015.

Figures

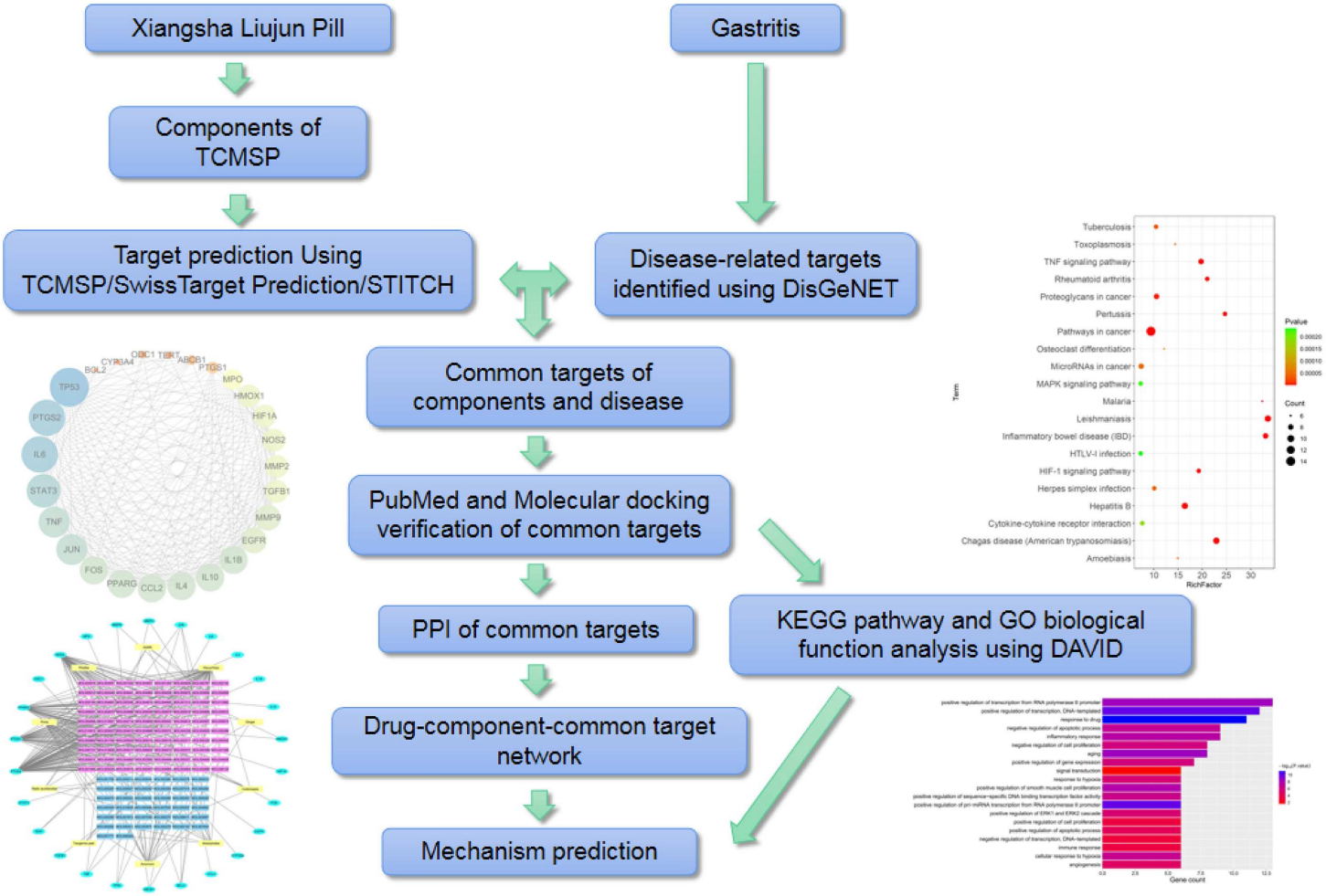

Figure 1

Complete workflow of this study.

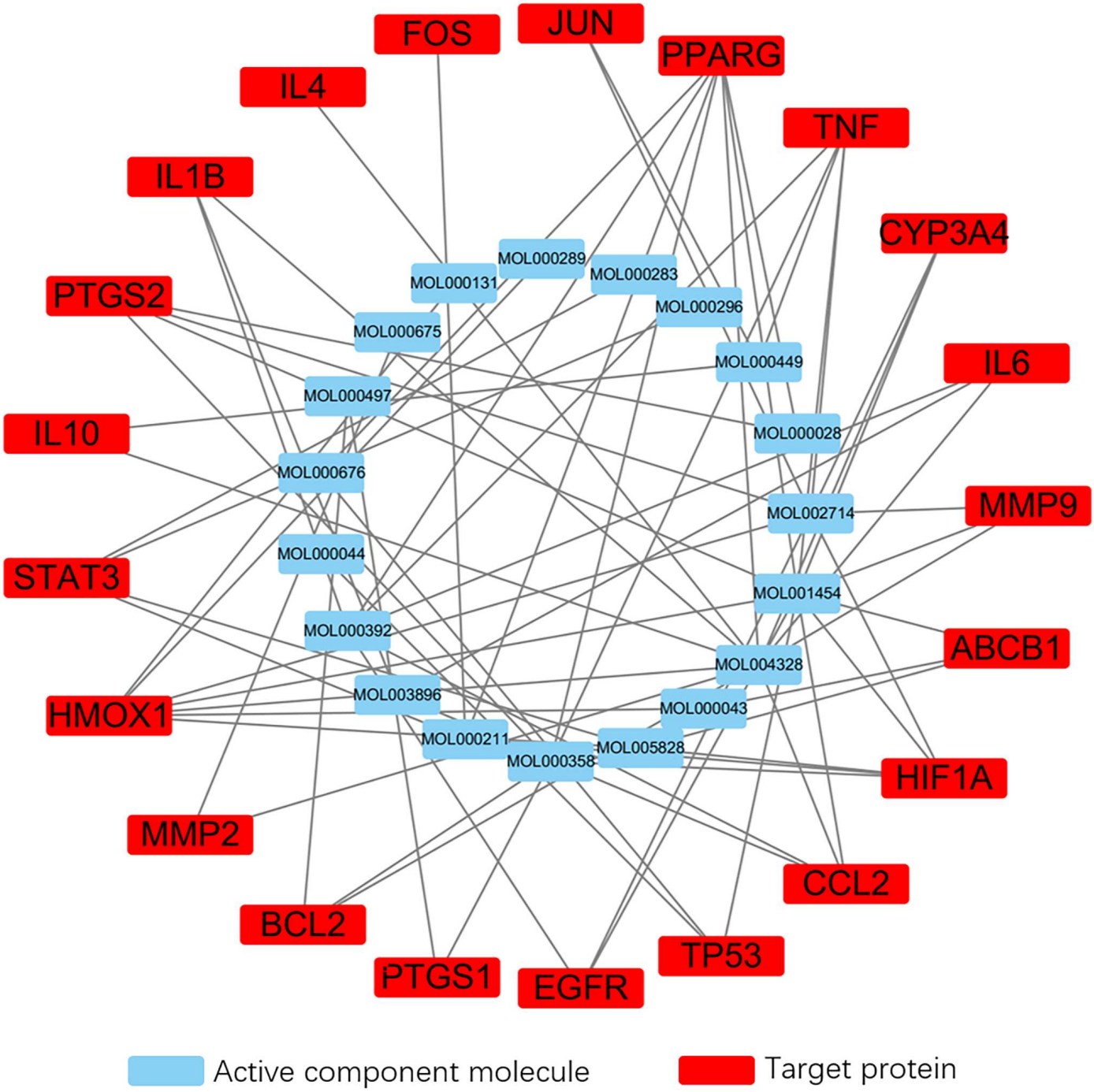

Figure 2

Network diagram of 21 verified targets and their corresponding active components.

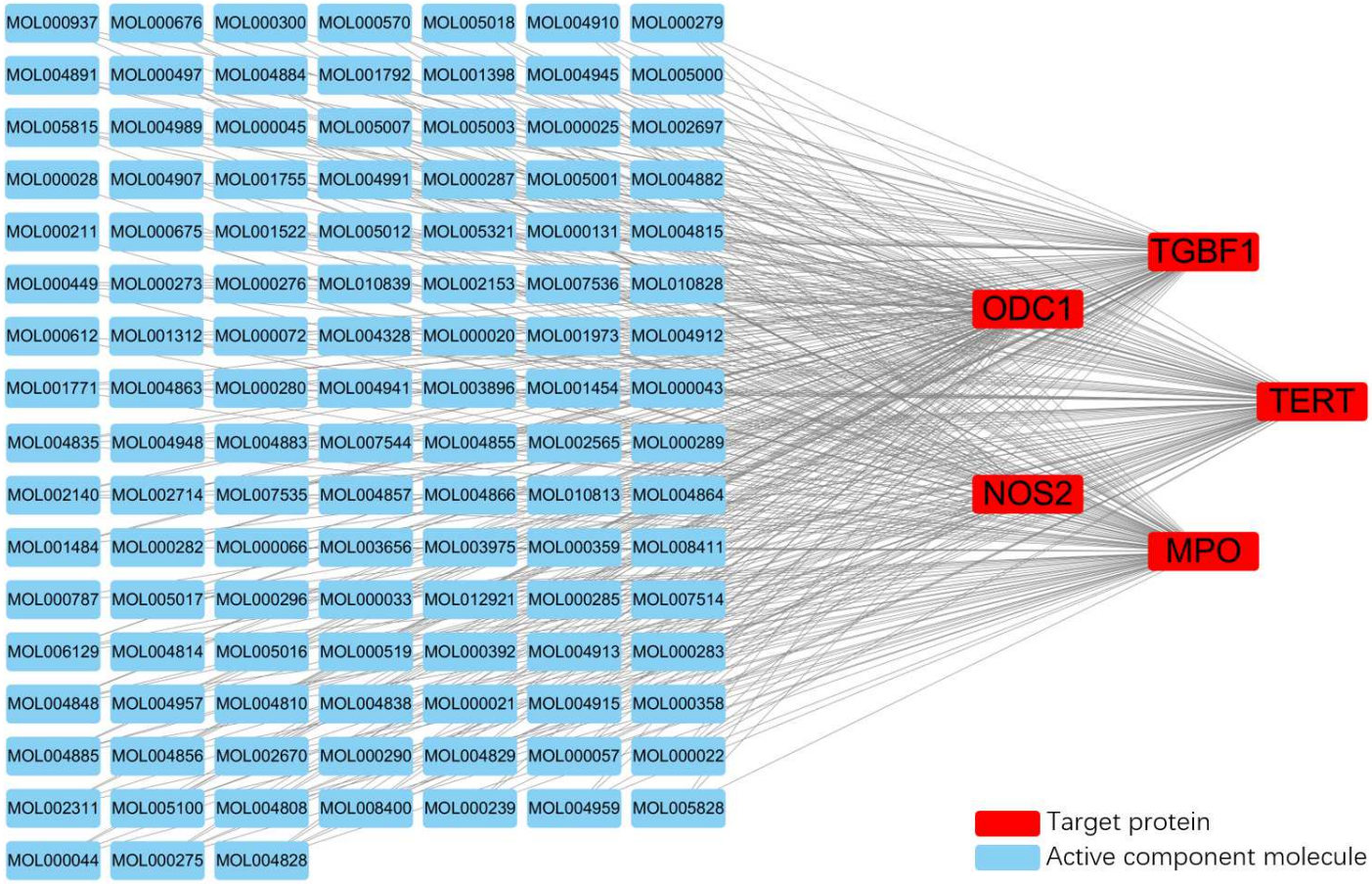

Figure 3

Network diagram of five unverified targets and active component molecules that can be successfully docked with the target in the LibDock mode.

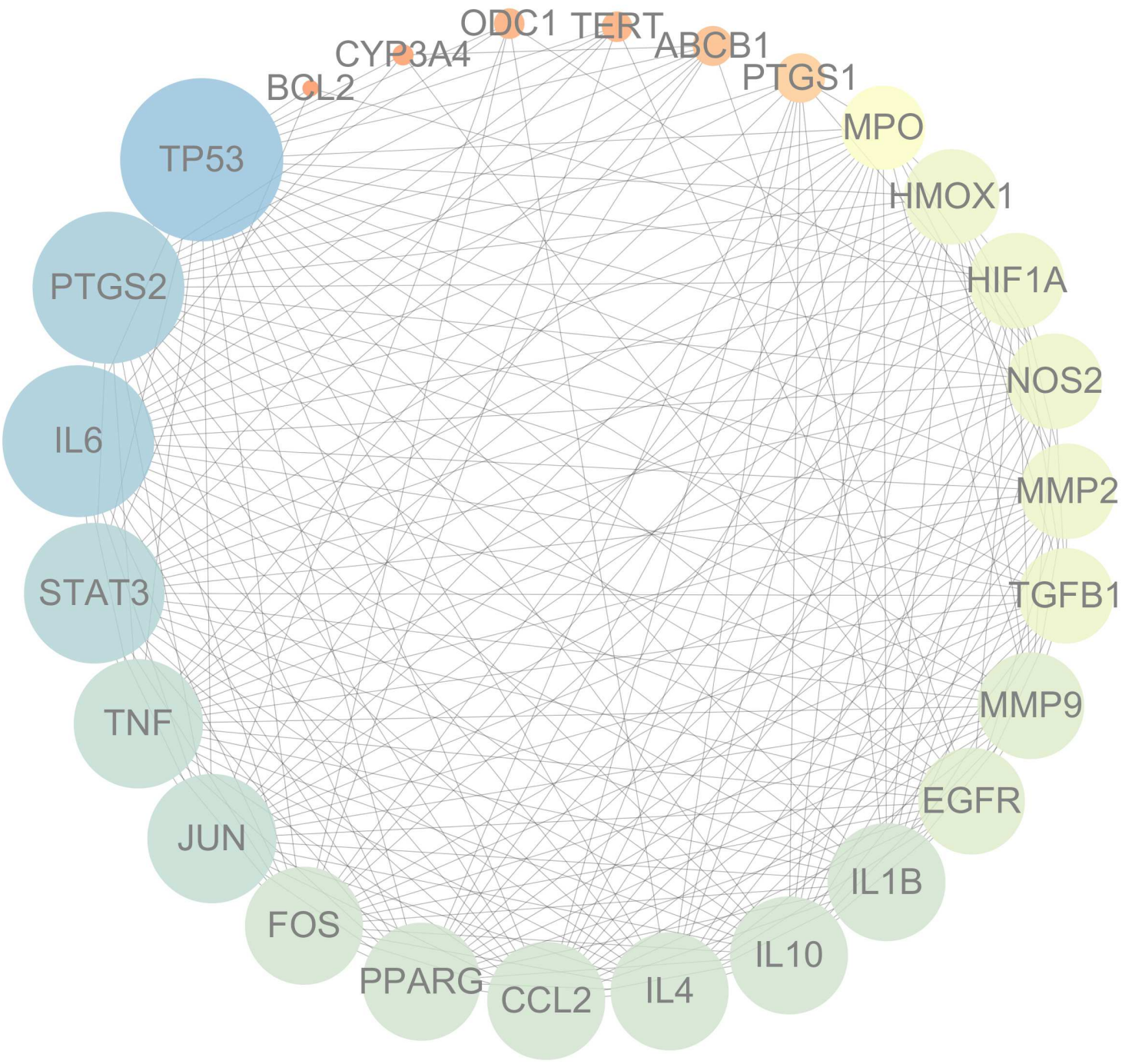

Figure 4

Protein-protein interaction network (PPI) diagram of the 26 common targets.

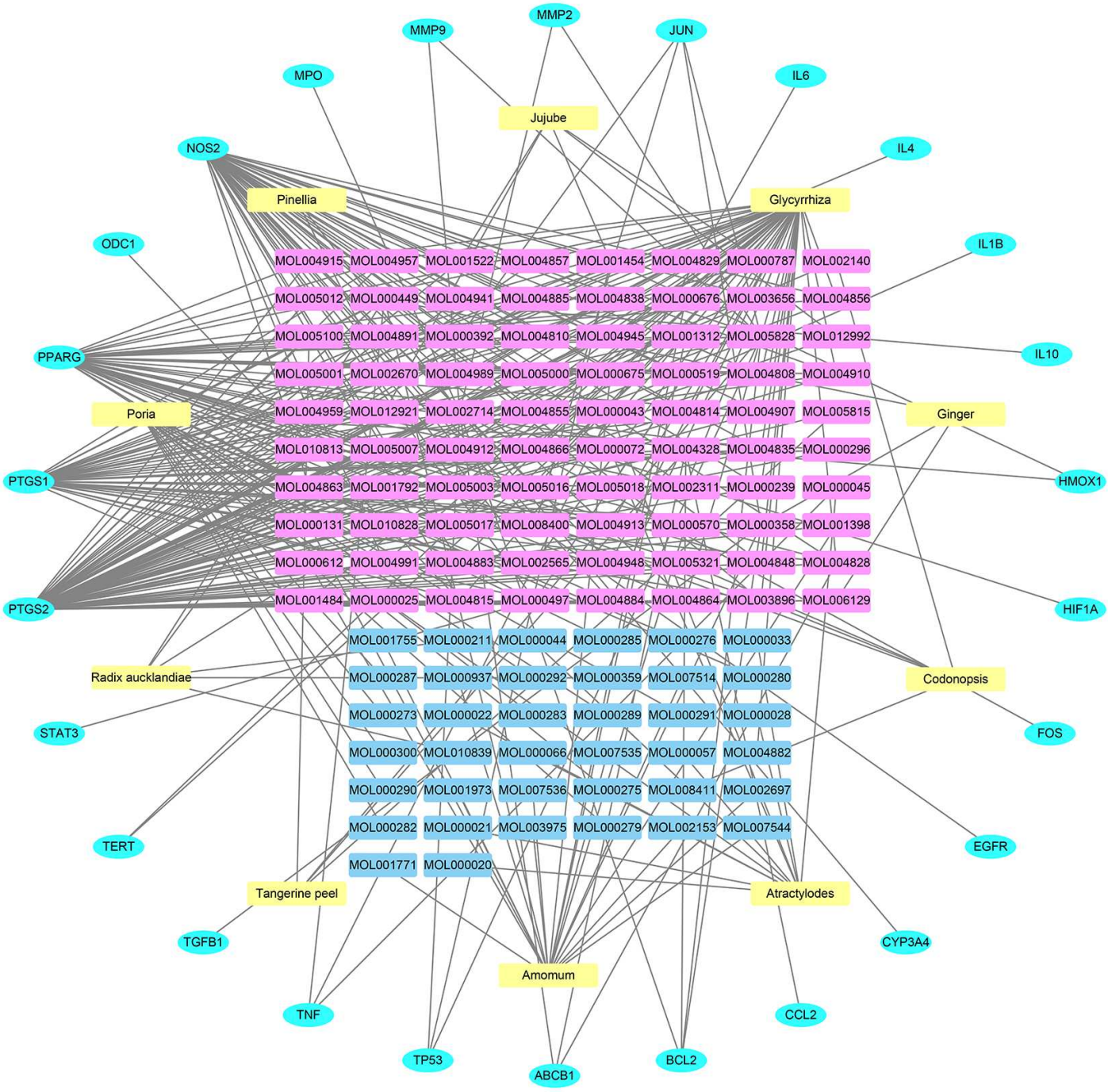

Figure 5

‘Drug-component-common target’ network diagram.

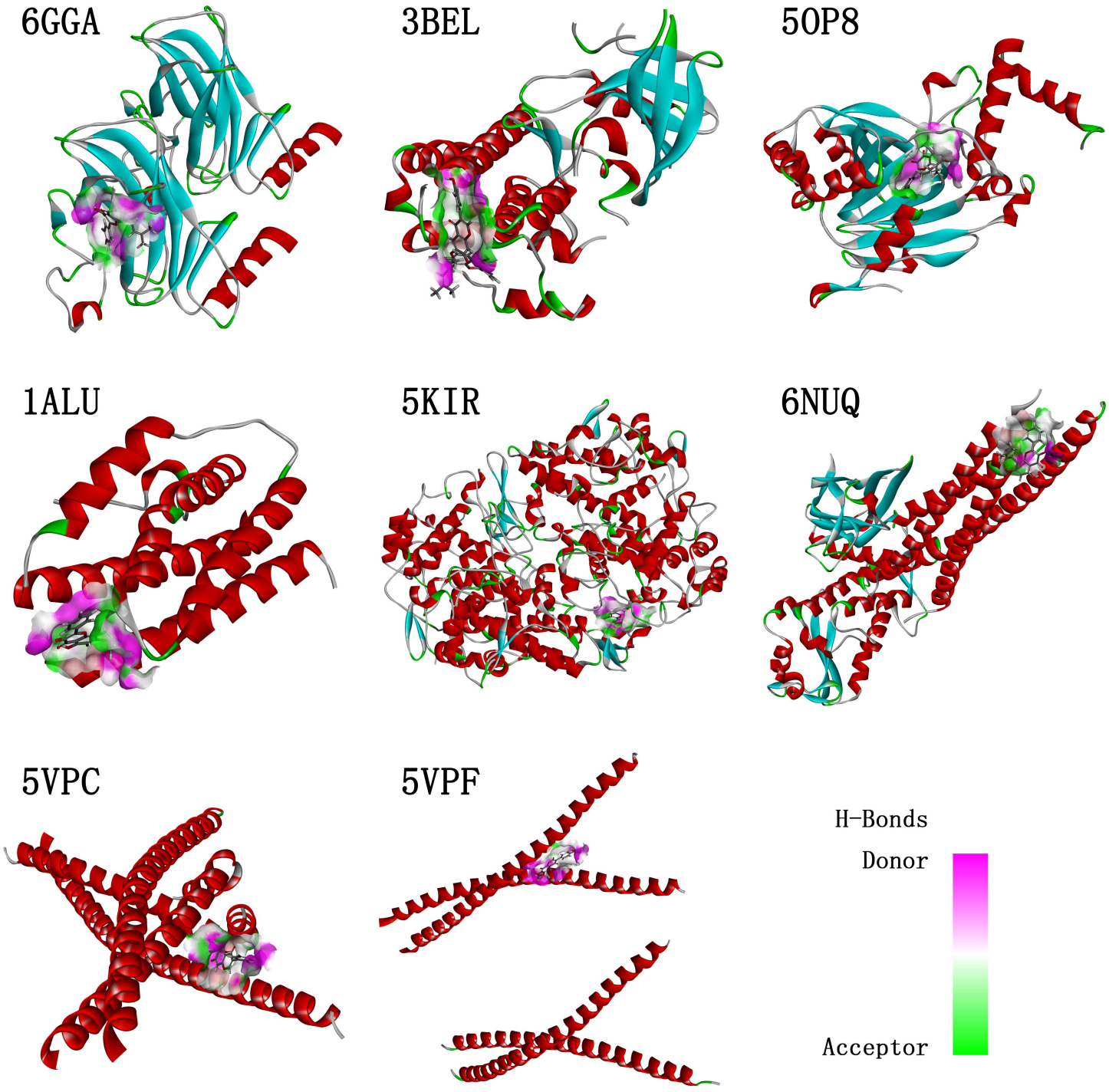

Figure 6

3D images of the docking poses between the eight key targets and their corresponding active components with the lowest binding energies under the CDOCKER flexible docking model.

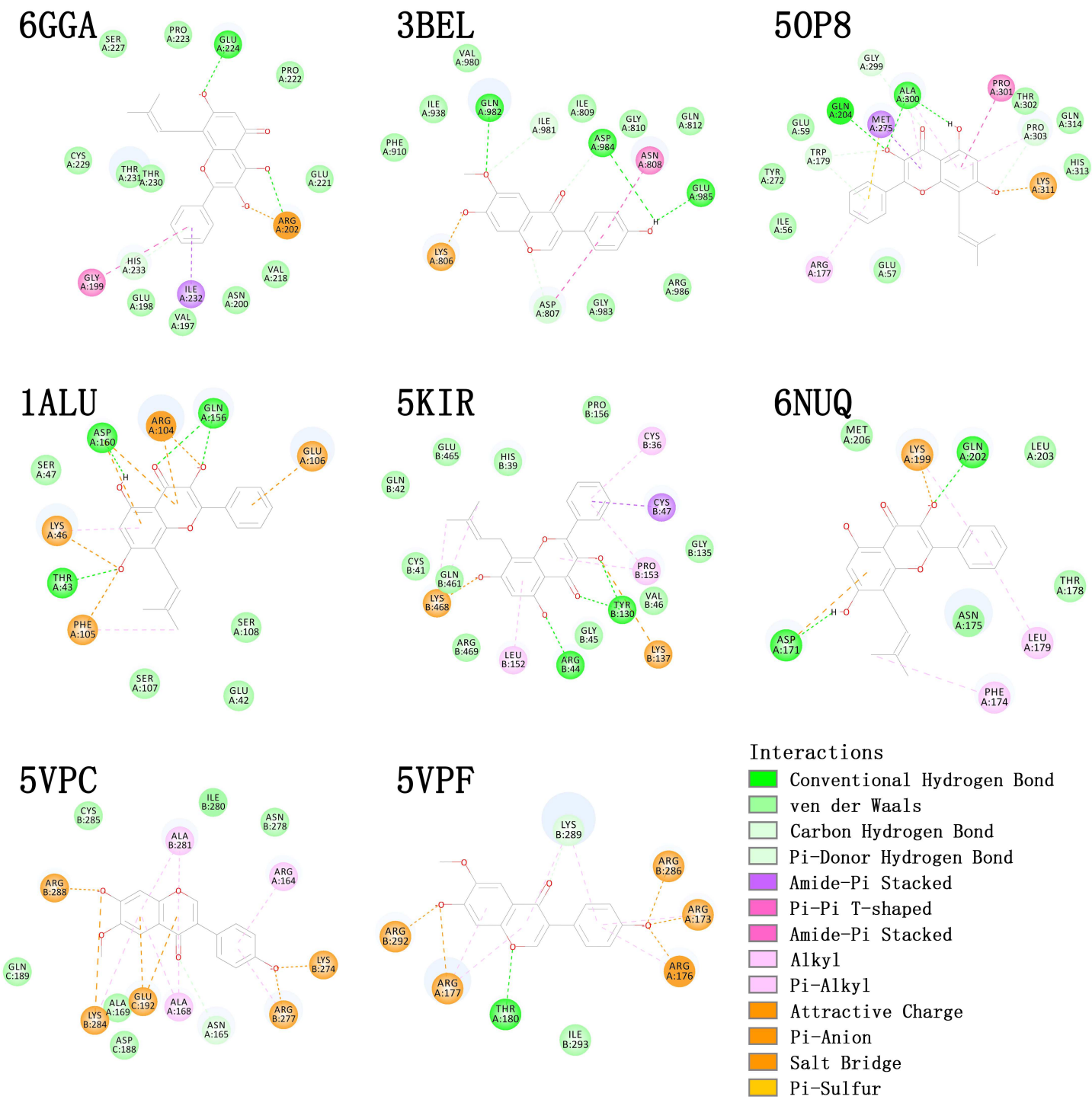

Figure 7

2D images of the docking poses between the eight key targets and their corresponding active components with the lowest binding energies under the CDOCKER flexible docking model.

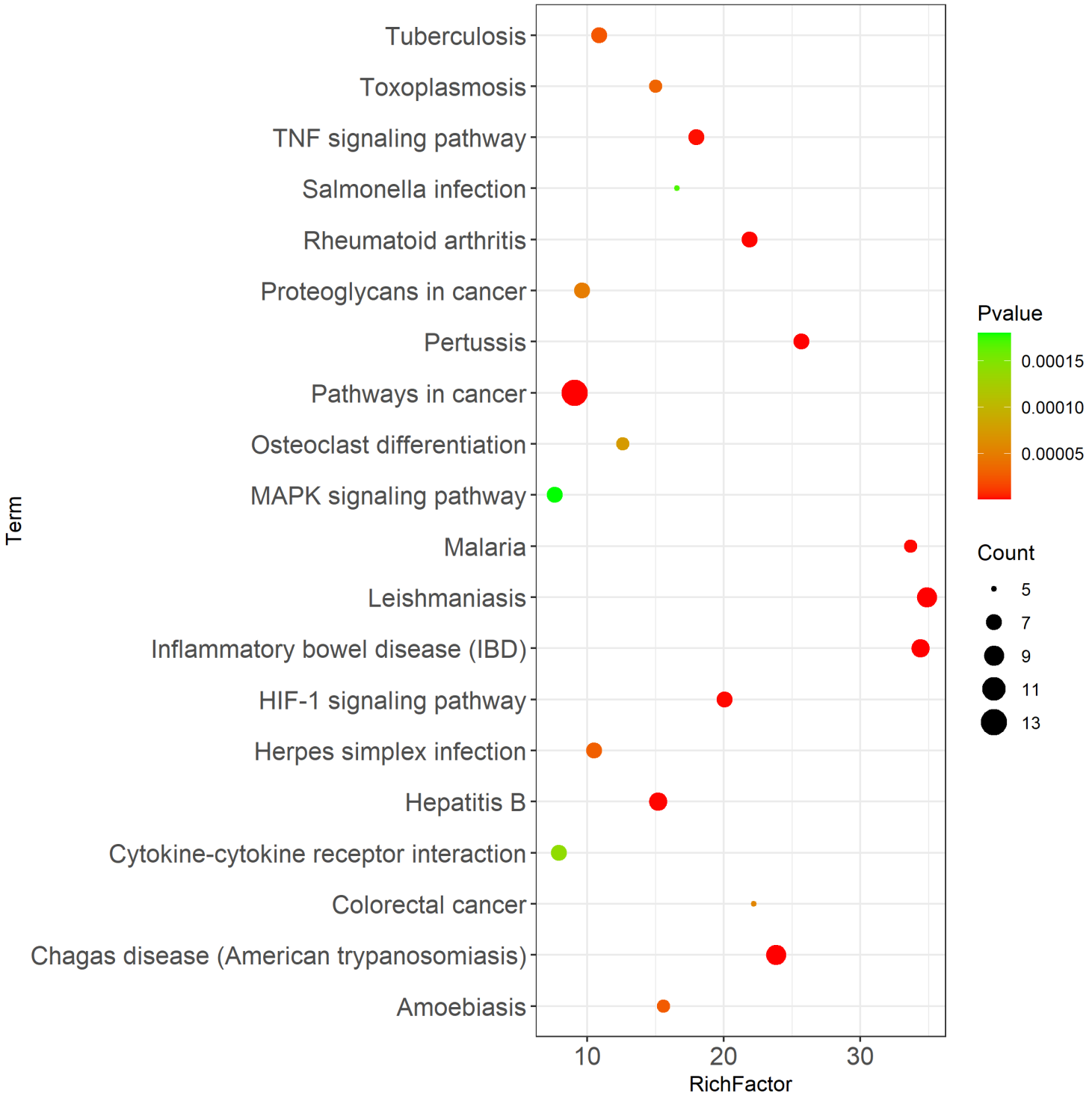

Figure 8

Bubble plot of the top 20 pathways obtained from the KEGG enrichment analysis.

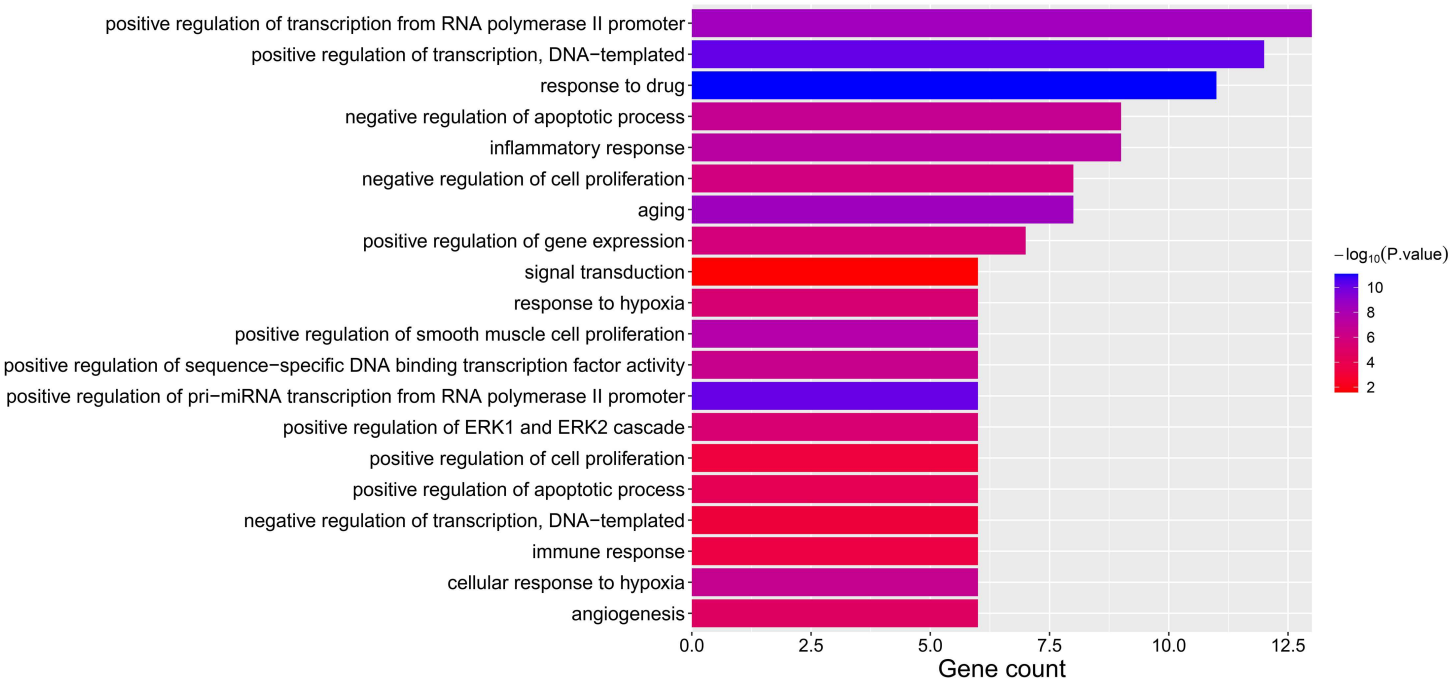

Figure 9

Bar plot of the top 20 biological processes obtained from the GO biological function analysis.

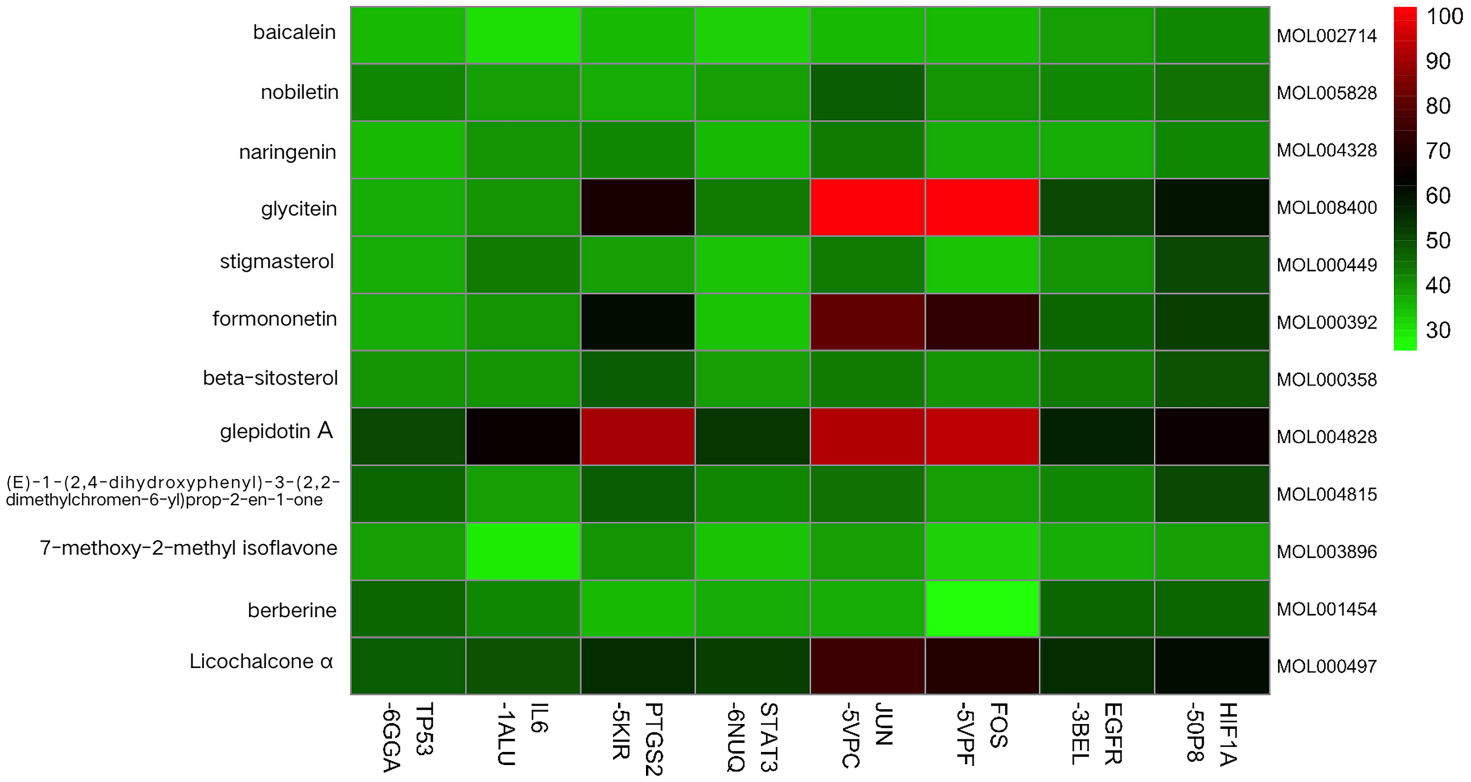

Figure 10

Heatmap displaying the docking scores between the 12 key components and eight hub targets.

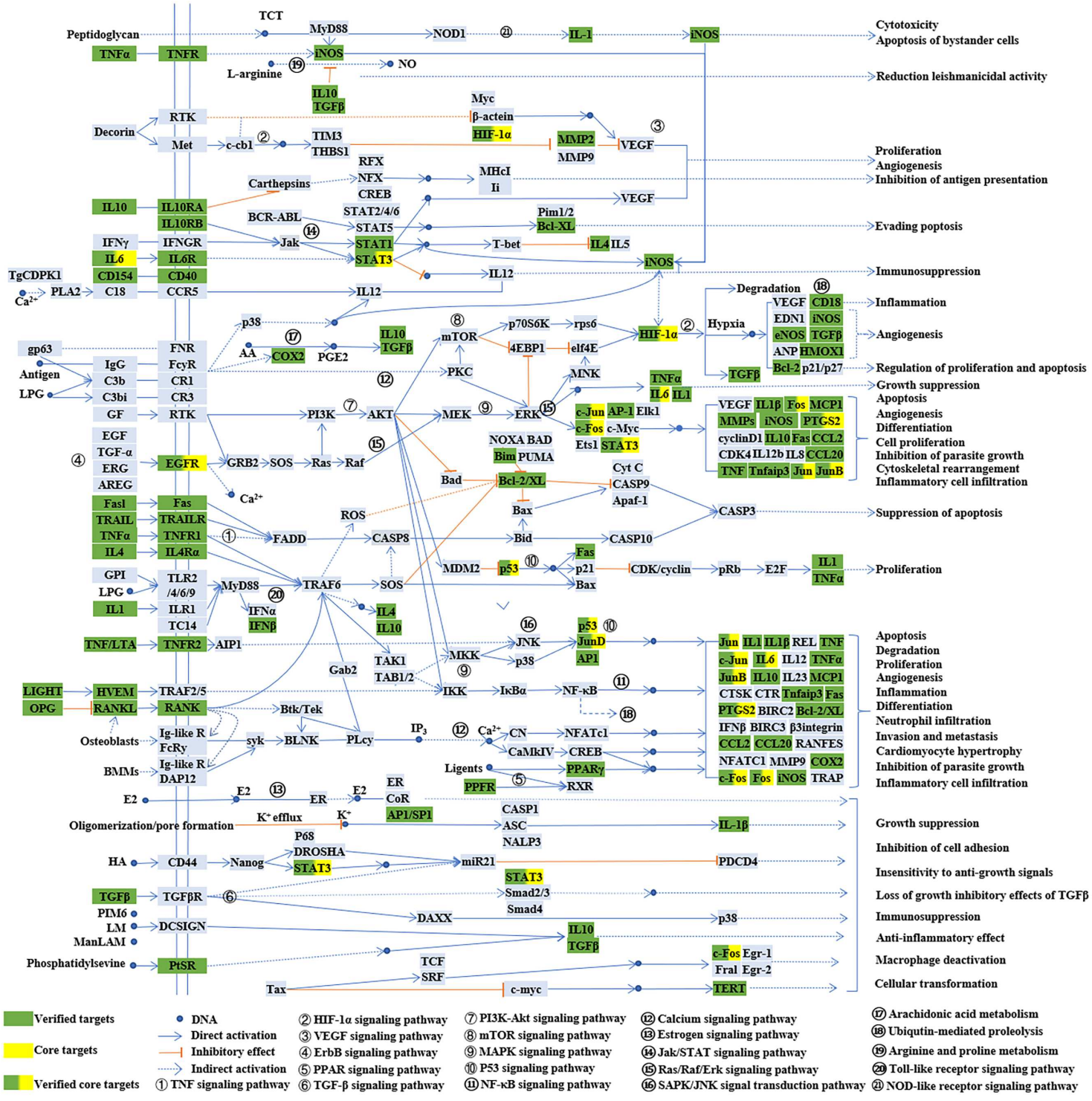

Figure 11

Complete signaling pathways identified from the exploration of the potential mechanism of XSLJP in the treatment of gastritis.

Supplementary Files

This is a list of supplementary files associated with this preprint. Click to download.

- SupplementaryMaterials.docx